EMMI Workshop

Understanding light (anti-)nuclei production at RHIC and LHC

Production of (anti)(hyper)nuclei via coalescence and kinetic approach

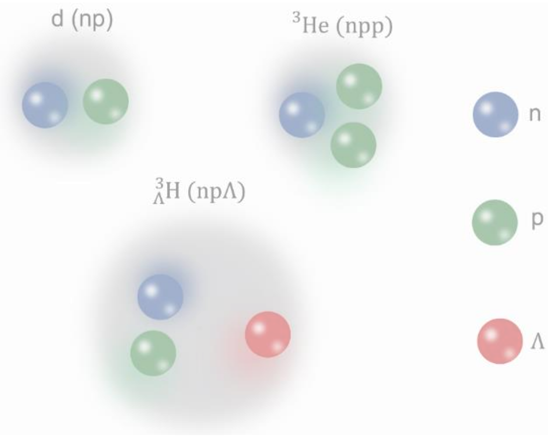

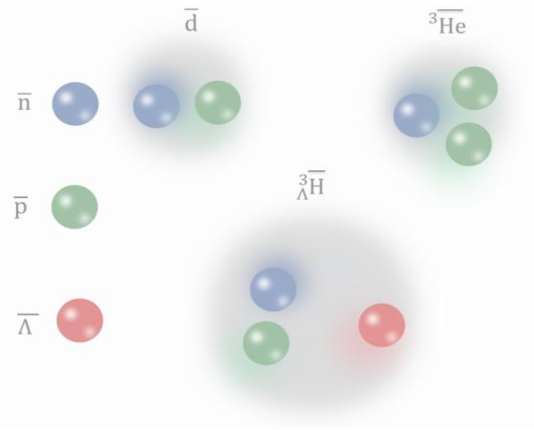

KaiJia Sun (孙开佳)
kjsun@fudan.edu.cn;
Institute of Modern Physics
Fudan University, China

Outline

1. Little-bang nucleosynthesis
2. Hypernuclei production from coalescence
3. Exotic particle production from coalescence
4. Effects of hadronic re-scatterings via the kinetic approach
5. Mott effects at large baryon densities
6. Discussion and summary

Little-Bang Nucleosynthesis

Big-Bang Nucleosynthesis (1)

K. A. Olive et al., Phys. Rept. 333, 389–407 (2000);

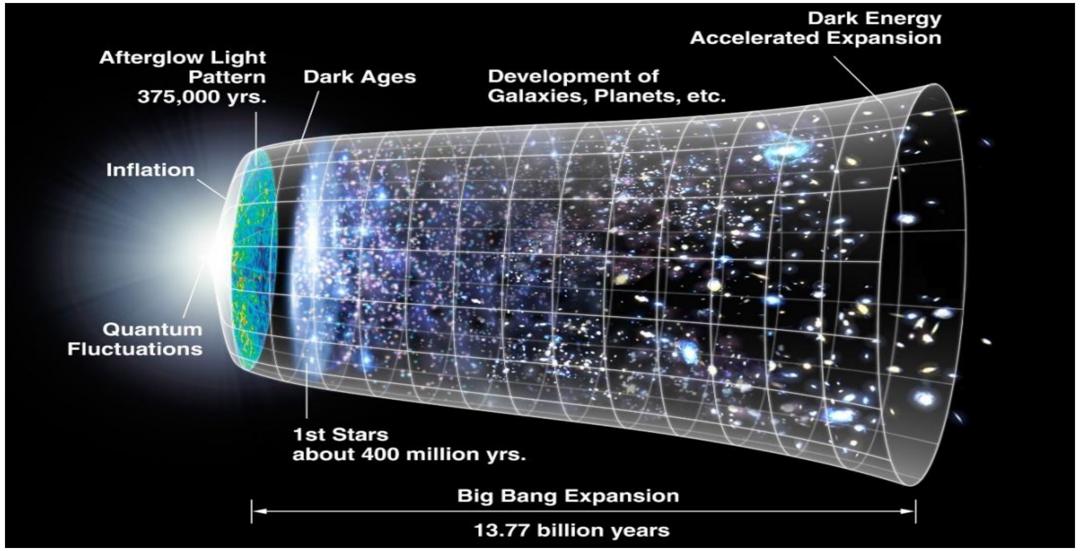

Big-bang nucleosynthesis is responsible for the formation of light nuclei (e.g., d, ^3He, ^4He) in our Universe. $t \sim 100\ s, kT \sim$ a few MeV

《The First Three Minutes》 S. Weinberg

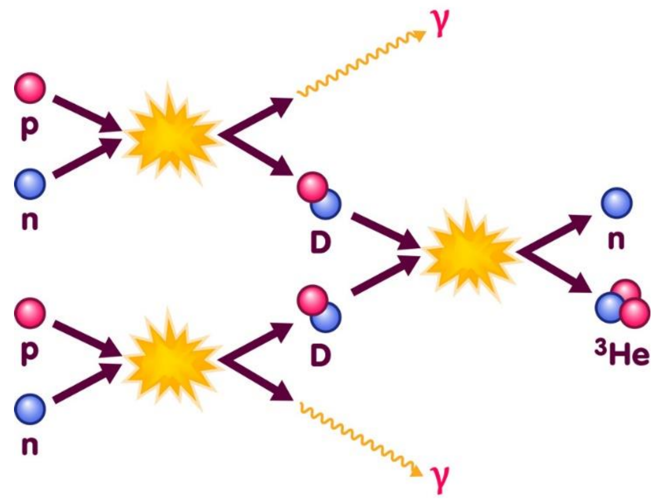

$$p + n \longrightarrow D + \gamma$$
$$D + p \longrightarrow {}^3He + \gamma$$
$$D + D \longrightarrow {}^3He + n$$
$$D + D \longrightarrow {}^3H + p$$
$${}^3He + n \longrightarrow {}^3H + p$$
$$D + D \longrightarrow {}^4He + \gamma$$
$${}^3He + D \longrightarrow {}^4He + p$$
$${}^3H + D \longrightarrow {}^4He + n.$$

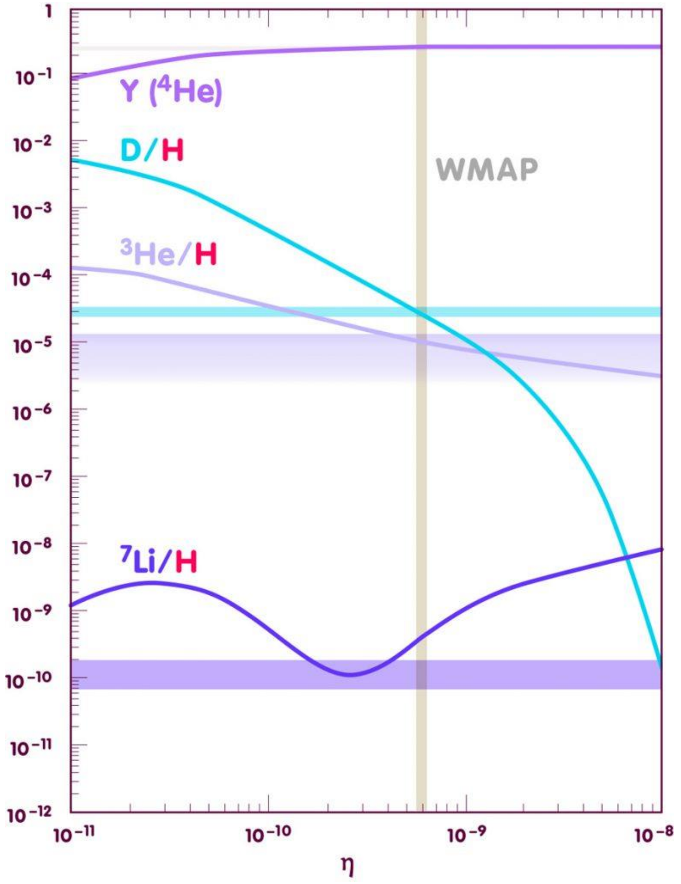

Little-Bang Nucleosynthesis (2)

Synthesis of antimatter nuclei

STAR (Nature 473,353(2011))

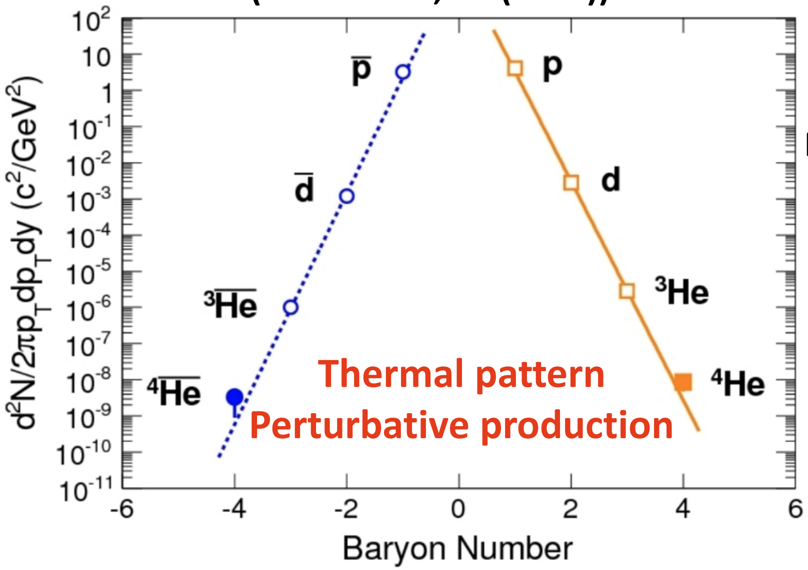

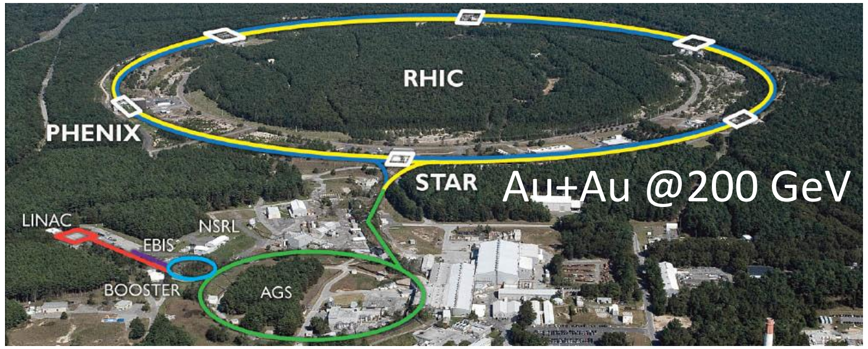

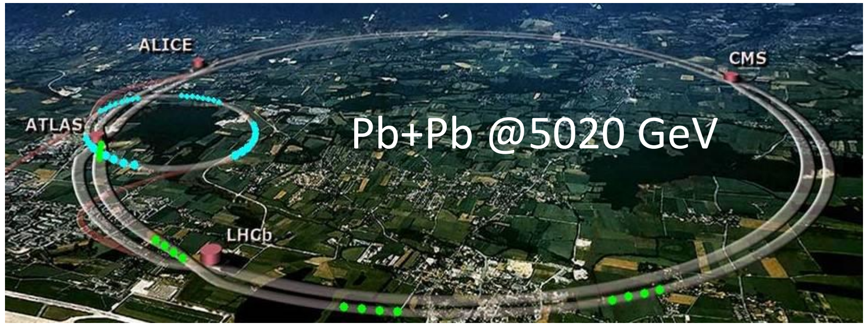

HADES

GSI

Matter-antimatter asymmetry

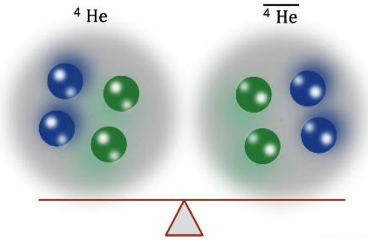

STAR (2310.12674)

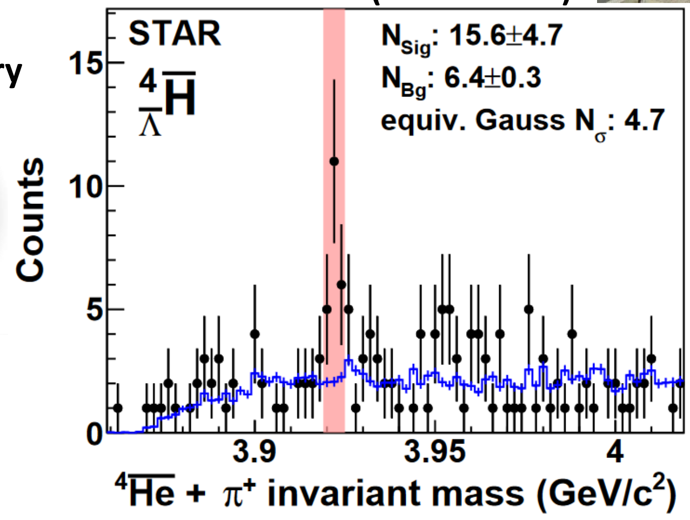

ALICE (QM2023)

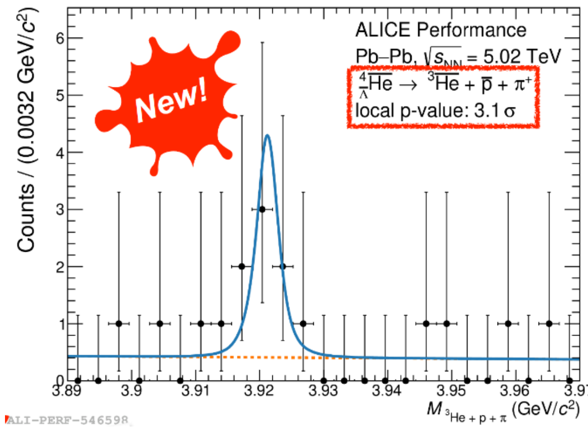

J. Chen et al., Phys. Rep. 760, 1 (2018);P. Braun-Munzinger and B. Donigus NPA987, 144 (2019)

Little-Bang Nucleosynthesis (3)

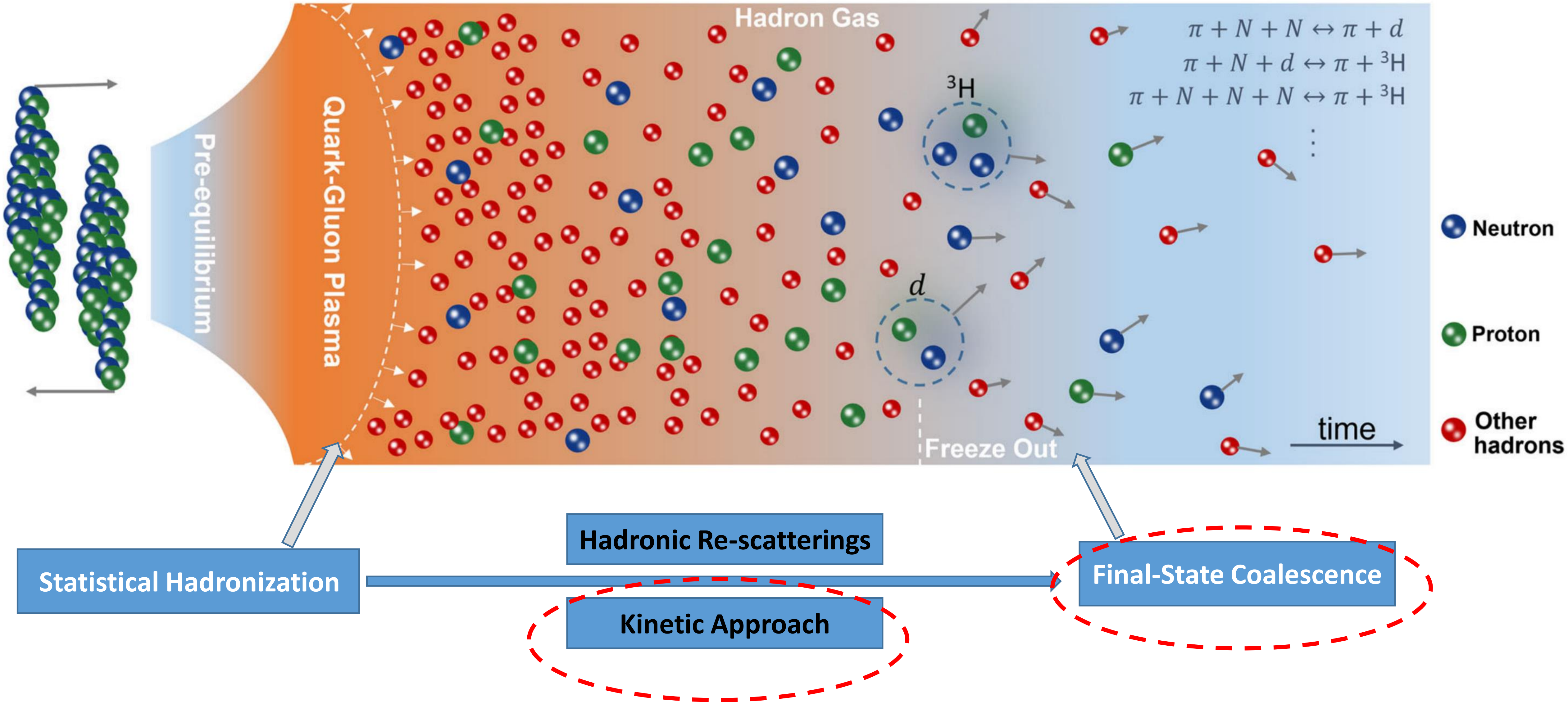

Kai-Jia Sun, Rui Wang, Che-Ming Ko, Yu-Gang Ma, and Chun Shen, Nat. Commun. 15, 1074 (2024)

Hypernuclei production from coalescence

Final-state coalescence (4)

1960s

Butler and Pearson, PR 129, 836 (1963):Two nucleons coalescence into a deuteron with the nuclear matter acting as a catalyzer

1970s

Gutbrod et al., PRL 37, 667 (1976); Coalescence parameter

$$E_A \frac{d^3 N_A}{dp_A^3} = B_A \left(E_p \frac{d^3 N_p}{dp_p^3} \right)^A$$

$$B_A = \left(\frac{4\pi}{3} p_0^3 \right)^{A-1} \frac{M}{m^A}, \; p_A = A p_p$$

1980s

Siemens & Kapusta, PRL 43, 1486 (1979)

$$\frac{S}{N} \approx 3.95 - \ln R_{\mathrm{dp}}$$

Gylassy, Frankel, and Remler, NPA 402, 596 (1983):

St. Mrówczyński, Phys. Lett. B 277, 43 (1992)

Coalescence & correlation

$$W = \frac{3}{4}(2\pi)^3 \int d^3\mathbf{r}\, D_r(\mathbf{r}) |\varphi(\mathbf{r})|^2 \qquad C(\mathbf{q}) = \int d^3\mathbf{r}\, D_r(\mathbf{r}) |\varphi_{\mathbf{q}}(\mathbf{r})|^2$$

1990s

Kahana et al., PRC 54, 388 (1996); AGS energies.

R. Scheibl and U. W. Heinz, PRC59. 1585(1999). **Quantum correction:**

$$\langle \mathcal{C}_d \rangle \approx \frac{1}{\left(1+\left(\frac{d}{2\mathcal{R}_\perp(m)}\right)^2\right)\sqrt{1+\left(\frac{d}{2\mathcal{R}_\parallel(m)}\right)^2}}$$

2010s-2020s

Zhang & Ko, PLB 780, 191 (2018)

Sun, Ko & Doenigus, PLB 792, 132 (2019)

$$\frac{N_d}{N_p} \approx \frac{3N_n}{4(mT_K R^2)^{3/2}} \frac{1}{1+\frac{2r_d^2}{3R^2}}$$

Sun, Chen, Ko & Xu, PLB 774, 103 (2017); 781, 499 (2018);816, 136258(2021). **Density fluc./corr.**

$$\frac{N_t N_p}{N_d^2} \approx \frac{1}{2\sqrt{3}}\left[1 + \Delta\rho_n + \frac{\lambda}{\sigma} G\left(\frac{\xi}{\sigma}\right)\right]$$

2010s-2020s

Zhao et al.,PRC98, 054905(2018):Hydro+UrQMD+Coal

Mrowczynski, EPJ.ST 229,3559(2020)

Blum, PRC99,044913(2019);Bellini et al., PRC103,014907:coalescence & correlation

Bellini and Kalweit, PRC 99, 054905 (2019).

Mahlein et al., EPJC 83, 804 (2023): realistic WF.

Many more …

Final-state coalescence (5)

R. Scheibl and U. W. Heinz, PRC59. 1585(1999);

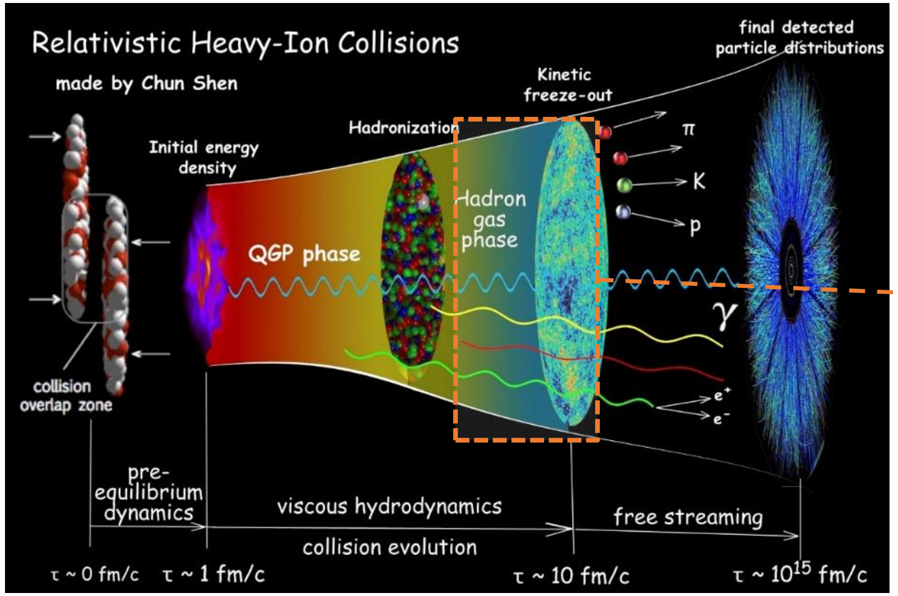

Coalescence Model

Deuteron

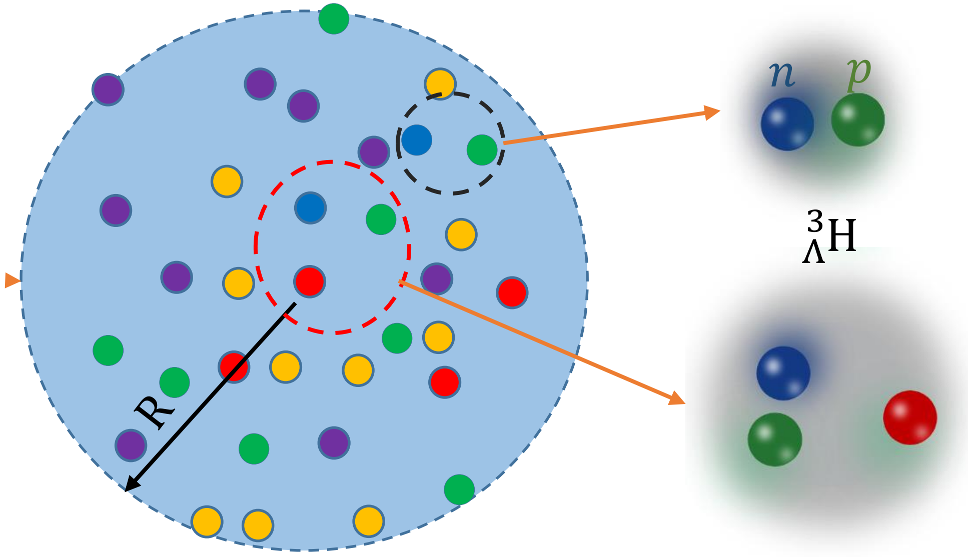

Density Matrix Formulation (sudden approximation)

$$N_A = Tr(\hat{\rho}_s \hat{\rho}_A)$$
$$= g_c \int d\Gamma\, \rho_s(\{x_i, p_i\}) \times W_A(\{x_i, p_i\})$$

Wigner function of light cluster

Overlap between source distribution function and Wigner function of light nuclei

Two-body coalescence $a + b \to c$:

$$N_c = \frac{2J_c+1}{(2J_a+1)(2J_b+1)} \int \frac{dx_a dk_a}{(2\pi)^3} \frac{dx_b dk_b}{(2\pi)^3} f_a(x_a,k_a) f_b(x_b,k_b) W_c(x,k)$$

$$\approx \frac{2J_c+1}{(2J_a+1)(2J_b+1)} \frac{N_a N_b}{\left(\frac{m_a m_b T}{m_a+m_b}(R_a^2+R_b^2)\right)^{3/2}} \times \boxed{\frac{1}{\left(1+\frac{\sigma^2}{R_a^2+R_b^2}\right)^{3/2}}}$$

“Quantum mechanical correction”

$$f_a = \frac{N_a}{(m_a T R_a^2)^{3/2}} e^{-\frac{k_a^2}{2m_a T} - \frac{x_a^2}{2R_a^2}} \qquad W_c = 8e^{-x^2/\sigma^2 - \sigma^2 k^2}$$

$$N_a = \int \frac{dx_a dk_a}{(2\pi)^3} f_a(x_a,k_a) \qquad 1 = \int \frac{dx dk}{(2\pi)^3} W_c(x,k)$$

$$N_d \propto \frac{1}{\left[1+\left(\frac{2r_d^2}{3R^2}\right)\right]^{\frac{3}{2}}}$$

Production — Structure

$$N_{^3_\Lambda H} \propto \frac{1}{\left[1+\left(\frac{r^2_{^3_\Lambda H}}{2R^2}\right)\right]^3}$$

can be inferred from Femtoscopy

K. J. Sun, C. M. Ko and B. Dönigus, PLB 792, 132 (2019)

Quantum Correction from Coalescence (6)

$$N_d \propto \frac{1}{\left[1+\left(\frac{2r_d^2}{3R^2}\right)\right]^{\frac{3}{2}}}$$

Production

Structure

$$N_{^3_\Lambda \mathrm{H}} \propto \frac{1}{\left[1+\left(\frac{r^2_{^3_\Lambda \mathrm{H}}}{2R^2}\right)\right]^{3}}$$

can be inferred from Femtoscopy

$$\frac{N_d}{N_p} \approx \frac{4.0\times 10^{-3}}{[1+\frac{2r_d^2}{3R^2}]^{3/2}} \qquad \frac{N_{^3He}}{N_p} \approx \frac{7.1\times 10^{-6}}{[1+\frac{r^2_{^3He}}{2R^2}]^{3}}$$

$$\frac{N_{^3_\Lambda H}}{N_\Lambda} \approx \frac{7.1\times 10^{-6}}{[1+\frac{r^2_{^3_\Lambda H}}{2R^2}]^{3}}$$:3-body coal.

K. J. Sun, C. M. Ko, and B. Dönigus, Phys. Lett. B792, 132-137(2019)

ALICE Results（ $^3_\Lambda$H ）

Phys. Rev. Lett. 128, 055203(2022)

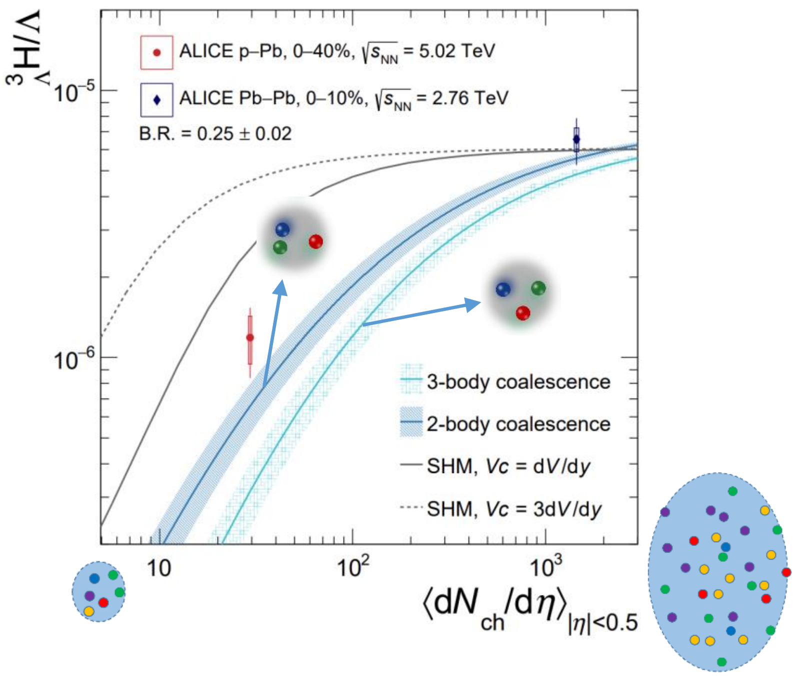

R. Scheibl and U. W. Heinz, PRC59. 1585(1999);
F. Bellini et al., PRC99,054905(2019);
K. J. Sun, C. M. Ko and B. Dönigus, PLB 792, 132 (2019);

How about the spectrum? (7)

MUSIC + UrQMD + Coalescence

Due to small lambda separation energy, the hypertriton can be well approximated as a bound state of deuteron and lambda hyperon.

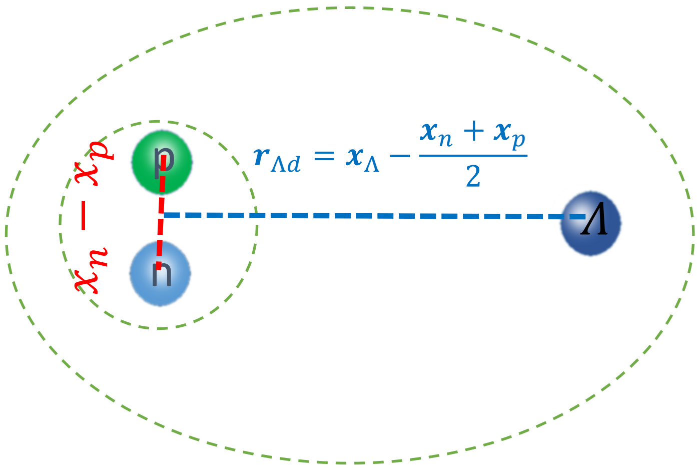

$$W_{ht} = 8^2 e^{-\frac{\boldsymbol{x}_1{}^2}{\sigma_1{}^2} - \boldsymbol{k}_1{}^2 \sigma_1{}^2 - \frac{\boldsymbol{x}_2{}^2}{\sigma_2{}^2} - \boldsymbol{k}_2{}^2 \sigma_2{}^2}$$

$$\boldsymbol{x}_1 = \frac{\boldsymbol{x}_n - \boldsymbol{x}_p}{\sqrt{2}}$$

$$\boldsymbol{k}_1 = \sqrt{2}\frac{m_p \boldsymbol{k}_n - m_n \boldsymbol{k}_p}{m_n + m_p}$$

$$\boldsymbol{x}_2 = \sqrt{\frac{2}{3}}\left(\frac{m_n \boldsymbol{x}_n - m_p \boldsymbol{x}_p}{m_n + m_p} - \boldsymbol{x}_\Lambda\right)$$

$$\boldsymbol{k}_2 = \sqrt{\frac{3}{2}}\frac{m_\Lambda(\boldsymbol{k}_n + \boldsymbol{k}_p) - (m_n + m_p)\boldsymbol{k}_\Lambda}{m_n + m_p + m_\Lambda}$$

$\Lambda - d$ distance: $\sqrt{< r_{\Lambda d}{}^2 >} = \frac{3}{2}\sigma_2$

Faddeev equations

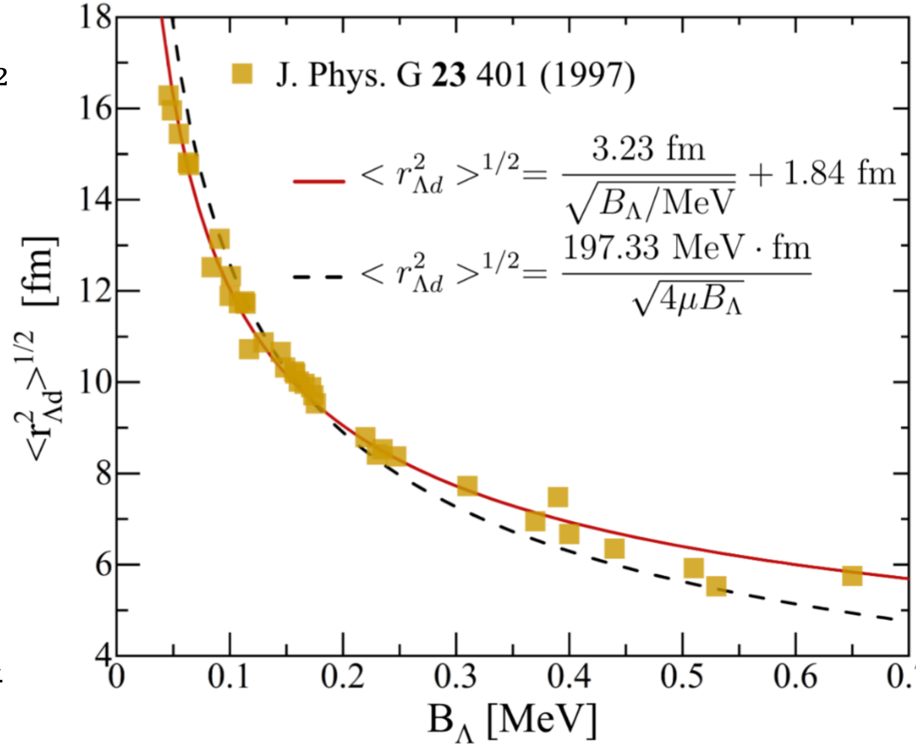

Taking $B_\Lambda = 0.13$ MeV

$\sqrt{< r_{\Lambda d}{}^2 >} \approx 10$ fm $\sigma_2 \approx 6.7$ fm

A. Cobis, A. S. Jensen, and D. V. Fedorov, J. Phys. G 23, 401 (1997)

Softening effect on hypertriton p_T spectrum (8)

D. N. Liu et al., arXiv:2404.02701(2024)

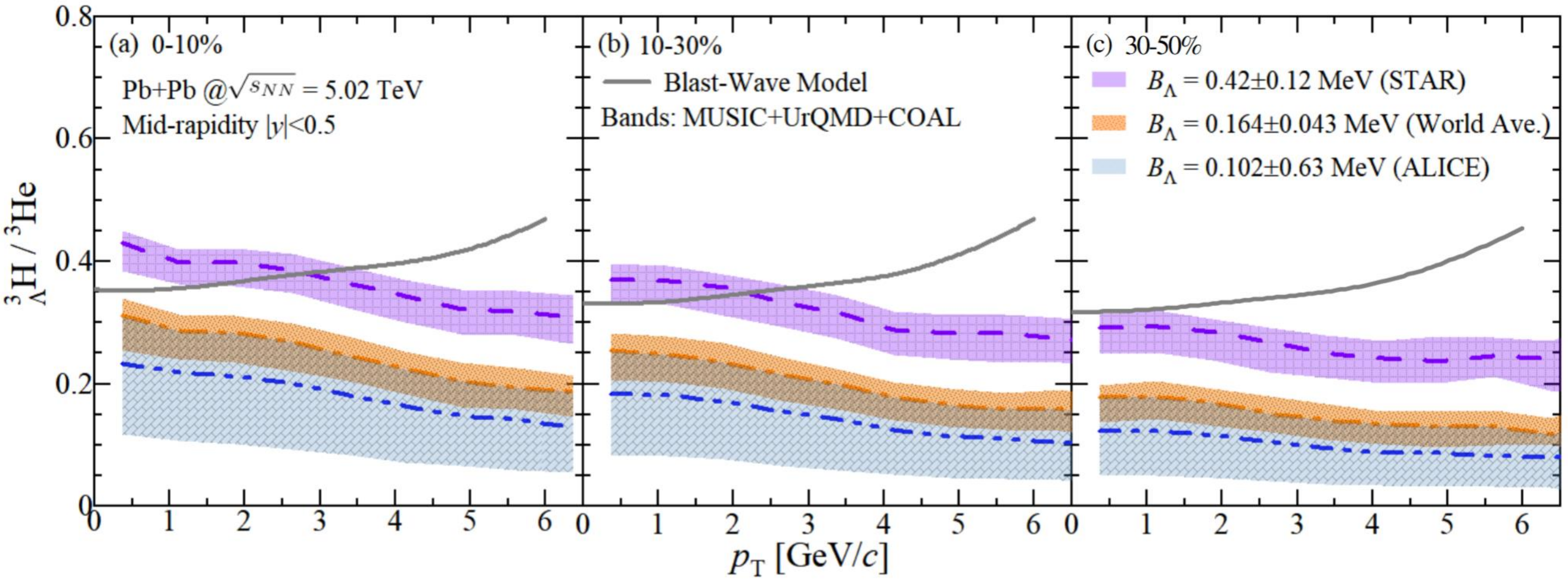

Two models yield opposite p_T dependence, even in the most central collisions!

Softening effect on hypertriton p_T spectrum (10)

Thermal effect (blast-wave model):

D. N. Liu et al., arXiv:2404.02701(2024)

$$f_{\rm BL} \propto \int m_T I_0\left(\frac{p_T \sinh(\rho)}{T_{\rm kin}}\right) K_1\left(\frac{m_T \cosh(\rho)}{T_{\rm kin}}\right) r dr.$$

$$\frac{f^{\rm ht}_{\rm BL}}{f^{\rm he3}_{\rm BL}} \propto \exp\left(-\frac{m^2_{\rm ht} - m^2_{\rm he3}}{(\sqrt{m^2_{\rm ht}+p_T^2} + \sqrt{m^2_{\rm he3}+p_T^2})T_{\rm eff}}\right) \qquad T_{\rm eff} = T_{\rm kin}\sqrt{\frac{1+\langle\beta_T\rangle}{1-\langle\beta_T\rangle}}$$

Coalescence:

$$\frac{f^{\rm ht}_{\rm COAL}}{f^{\rm he3}_{\rm COAL}} \approx \frac{f^{\rm ht}_{\rm BL}}{f^{\rm he3}_{\rm BL}} \times \frac{[1+\frac{\sigma^2_{\rm he3}}{2R^2(p_T)}]^3}{[1+\frac{\sigma_1^2}{2R^2(p_T)}]^{3/2}[1+\frac{\sigma_2^2}{2R^2(p_T)}]^{3/2}}$$

Competition between (collective) flow effects and quantum effects

$\mathcal{C}$

Thermal contribution: increases as increasing pt due to the flow effect

Quantum correction: decreases as increasing pt (since the inhomogeneity length R decreases)

Large source size limit:

$$\mathcal{C} \approx 1 - \frac{3(\sigma_2^2 + \sigma_1^2 - 2\sigma^2_{\rm he3})}{4R(p_T)^2}$$

Small source size limit:

$$\mathcal{C} \approx \frac{\sigma^6_{\rm he3}}{\sigma_1^6\sigma_2^6} \times \left[1 + 3R^2(p_T)\left(\frac{2}{\sigma^2_{\rm he3}} - \frac{1}{\sigma_1^2} - \frac{1}{\sigma_2^2}\right)\right]$$

Softening effect on hypertriton p_T spectrum (9)

D. N. Liu et al., arXiv:2404.02701(2024)

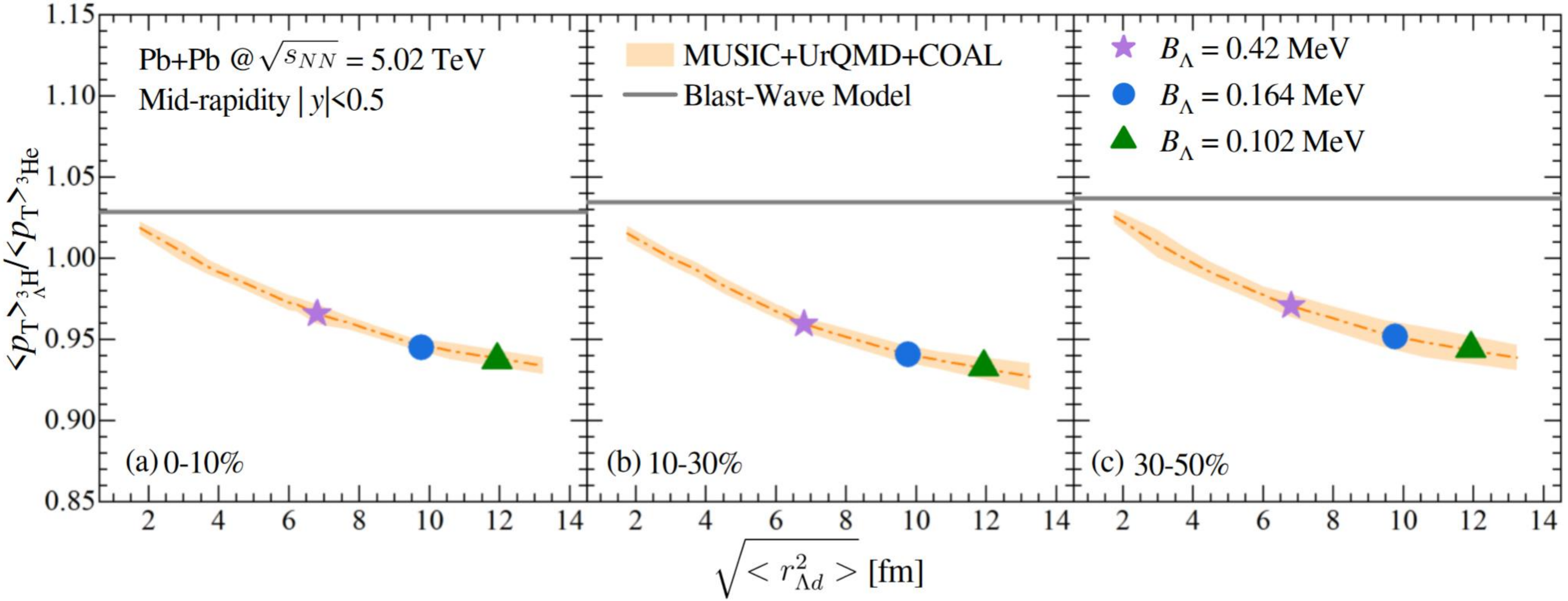

Sensitive to hypertriton internal wavefunction

Softening of hypertriton spectrum can be tested in experiments

Exotic particle production from coalescence

Physics Letters B 792 (2019) 284–289

Contents lists available at ScienceDirect

Physics Letters B

www.elsevier.com/locate/physletb

$N\Omega$ dibaryon from lattice QCD near the physical point

Takumi Iritani [a,*], Sinya Aoki [b], Takumi Doi [a,c], Faisal Etminan [d], Shinya Gongyo [a], Tetsuo Hatsuda [c,a], Yoichi Ikeda [e], Takashi Inoue [f], Noriyoshi Ishii [e], Takaya Miyamoto [b], Kenji Sasaki [b], HAL QCD Collaboration

[a] RIKEN Nishina Center (RNC), Saitama 351-0198, Japan
[b] Yukawa Institute of Theoretical Physics, Kyoto Univ., Kyoto 606-8502, Japan
[c] RIKEN Interdisciplinary Theoretical and Mathematical Sciences Program (iTHEMS), Saitama 351-0198, Japan
[d] Dept. of Phys., Faculty of Sciences, University of Birjand, Birjand 97175-615, Iran
[e] Research Center for Nuclear Physics (RCNP), Osaka Univ., Osaka 567-0047, Japan
[f] College of Bioresource Science, Nihon Univ., Kanagawa 252-0880, Japan

ARTICLE INFO

Article history:
Received 15 October 2018
Received in revised form 26 March 2019
Accepted 26 March 2019
Available online 2 April 2019
Editor: J. Hisano

Keywords:
Dibaryon
Lattice QCD
Hyperon interaction

ABSTRACT

The nucleon(N)-Omega(Ω) system in the S-wave and spin-2 channel ($^5S_2$) is studied from the (2+1)-flavor lattice QCD with nearly physical quark masses ($m_\pi \simeq 146$ MeV and $m_K \simeq 525$ MeV). The time-dependent HAL QCD method is employed to convert the lattice QCD data of the two-baryon correlation function to the baryon-baryon potential and eventually to the scattering observables. The $N\Omega(^5S_2)$ potential, obtained under the assumption that its couplings to the D-wave octet-baryon pairs are small, is found to be attractive in all distances and to produce a quasi-bound state near unitarity: In this channel, the scattering length, the effective range and the binding energy from QCD alone read $a_0 = 5.30(0.44)(^{+0.16}_{-0.01})$ fm, $r_{\rm eff} = 1.26(0.01)(^{+0.02}_{-0.01})$ fm, $B = 1.54(0.30)(^{+0.04}_{-0.10})$ MeV, respectively. Including the extra Coulomb attraction, the binding energy of $p\Omega^-(^5S_2)$ becomes $B_{p\Omega^-} = 2.46(0.34)(^{+0.04}_{-0.11})$ MeV. Such a spin-2 $p\Omega^-$ state could be searched through two-particle correlations in p-p, p-nucleus and nucleus-nucleus collisions.

PHYSICAL REVIEW LETTERS **120,** 212001 (2018)

Most Strange Dibaryon from Lattice QCD

Shinya Gongyo,[1] Kenji Sasaki,[1,2] Sinya Aoki,[1,2,3] Takumi Doi,[1,4] Tetsuo Hatsuda,[4,1] Yoichi Ikeda,[1,5] Takashi Inoue,[1,6] Takumi Iritani,[1] Noriyoshi Ishii,[1,5] Takaya Miyamoto,[1,2] and Hidekatsu Nemura[1,5]

(HAL QCD Collaboration)

[1] *RIKEN Nishina Center, RIKEN, Saitama 351-0198, Japan*
[2] *Center for Gravitational Physics, Yukawa Institute for Theoretical Physics, Kyoto University, Kyoto 606-8502, Japan*
[3] *Center for Computational Sciences, University of Tsukuba, Ibaraki 305-8571, Japan*
[4] *RIKEN iTHEMS Program, RIKEN, Saitama 351-0198, Japan*
[5] *Research Center for Nuclear Physics (RCNP), Osaka University, Osaka 567-0047, Japan*
[6] *Nihon University, College of Bioresource Sciences, Kanagawa 252-0880, Japan*

(Received 8 September 2017; revised manuscript received 6 March 2018; published 23 May 2018)

The $\Omega\Omega$ system in the $^1S_0$ channel (the most strange dibaryon) is studied on the basis of the $(2+1)$-flavor lattice QCD simulations with a large volume $(8.1\ \text{fm})^3$ and nearly physical pion mass $m_\pi \simeq 146$ MeV at a lattice spacing of $a \simeq 0.0846$ fm. We show that lattice QCD data analysis by the HAL QCD method leads to the scattering length $a_0 = 4.6(6)(^{+1.2}_{-0.5})$ fm, the effective range $r_{\rm eff} = 1.27(3)(^{+0.06}_{-0.03})$ fm, and the binding energy $B_{\Omega\Omega} = 1.6(6)(^{+0.7}_{-0.6})$ MeV. These results indicate that the $\Omega\Omega$ system has an overall attraction and is located near the unitary regime. Such a system can be best searched experimentally by the pair-momentum correlation in relativistic heavy-ion collisions.

DOI: 10.1103/PhysRevLett.120.212001

pΩ and ΩΩ

J. Pu, K. J. Sun, and L. W. Chen, arXiv:2402. 04185(2024)

$$E\frac{d^3N_c}{d^3P} = Eg_c\int\left(\prod_{i=1}^{M}\frac{d^3p_i}{E_i}d^4x_iS(x_i,p_i)\right)\times \rho_c^W(x_1,...,x_M;p_1,...,p_M)\delta^3(\mathbf{P}-\sum_{i=1}^{M}\mathbf{p_i}),$$

$$\rho_c^W(x_1,...,x_M;p_1,...,p_M) = \rho^W(q_1,\cdots,q_{M-1},k_1,\cdots,k_{M-1}) = 8^{M-1}\exp[-\sum_{i=1}^{M-1}(q_i^2/\sigma_i^2+\sigma_i^2k_i^2)],$$

FOPb-p						
Centrality	T(MeV)	ρ_0	R_0(fm)	τ_0(fm/c)	$\Delta\tau$	ξ_H
0-10%	95.94	1.28	19.53	15.36	1.0	38.55
10-20%	98.77	1.25	16.90	13.30	1.0	29.55
20-40%	103.74	1.21	13.68	10.77	1.0	19.00
40-60%	108.30	1.12	9.90	7.79	1.0	13.28
60-80%	114.42	1.01	6.37	5.01	1.0	8.50
FOPb-Ω						
Centrality	T(MeV)	ρ_0	R_0(fm)	τ_0(fm/c)	$\Delta\tau$	ξ_H
0-10%	95.94	1.08	19.53	15.36	1.0	643.19
10-20%	98.77	1.10	16.90	13.30	1.0	375.80
20-40%	103.74	1.04	13.68	10.77	1.0	174.88
40-60%	108.30	0.97	9.90	7.79	1.0	81.08
60-80%	114.42	0.95	6.37	5.01	1.0	19.73

Centrality	T(MeV)	ρ_0	R_0(fm)	τ_0(fm/c)	$\Delta\tau$	ξ_u	ξ_s
$0\sim10\%$	154	1.08	13.6	11.0	1.3	1.02	0.89
$10\sim20\%$	154	1.08	12.0	9.7	1.3	1.02	0.89
$20\sim40\%$	154	1.08	9.9	8.0	1.3	1.02	0.89
$40\sim60\%$	157	1.03	7.3	5.94	1.3	1.02	0.89
$60\sim80\%$	160	0.95	4.8	3.9	1.3	1.13	0.85

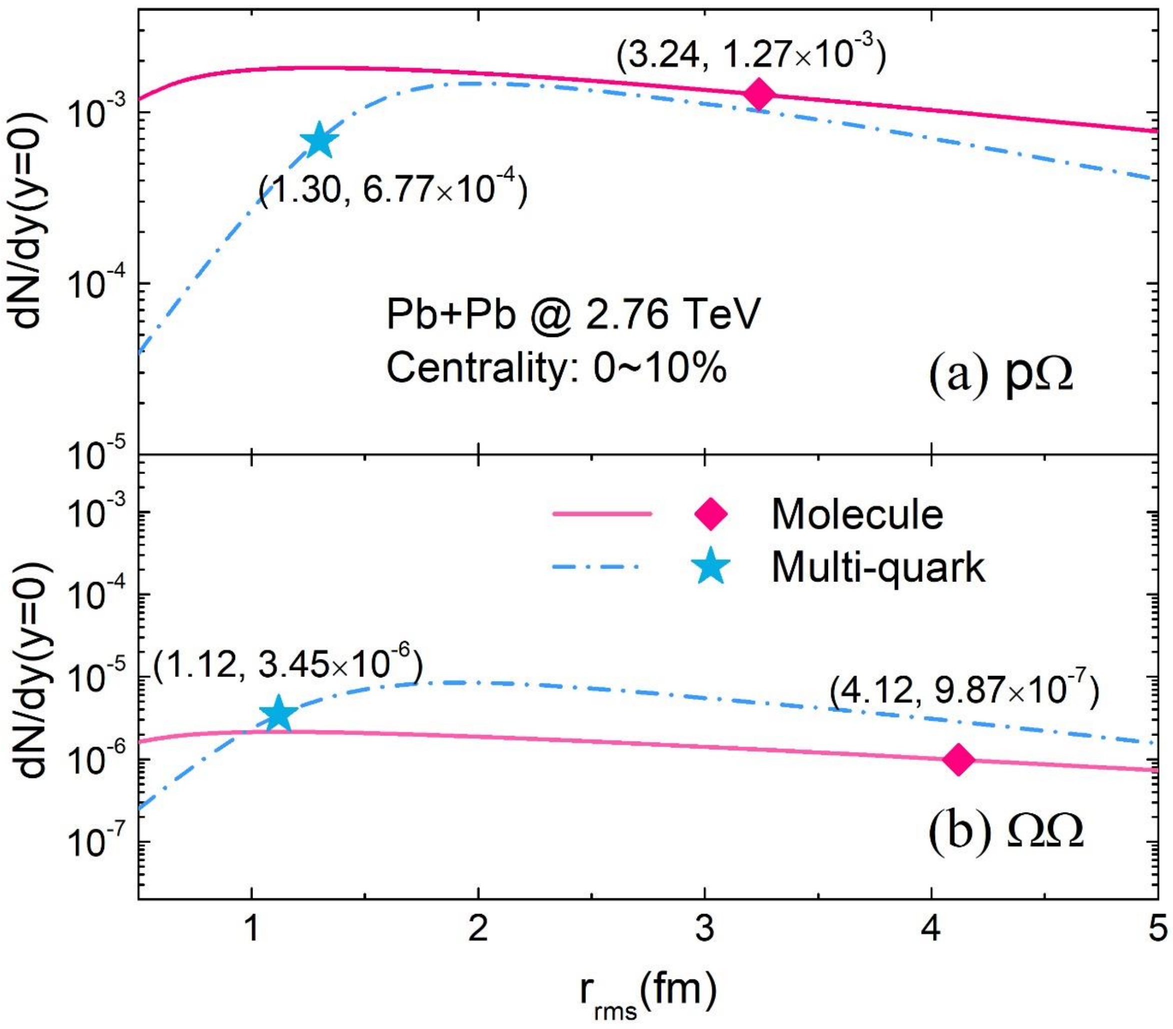

K. J. Sun and L. W. Chen, Phys. Lett. B 751, 272 (2015).
Song Zhang and Yu-Gang Ma, Phys. Lett. B 811 (2020) 135867

pΩ and ΩΩ

J. Pu, K. J. Sun, and L. W. Chen, arXiv:2402. 04185(2024)

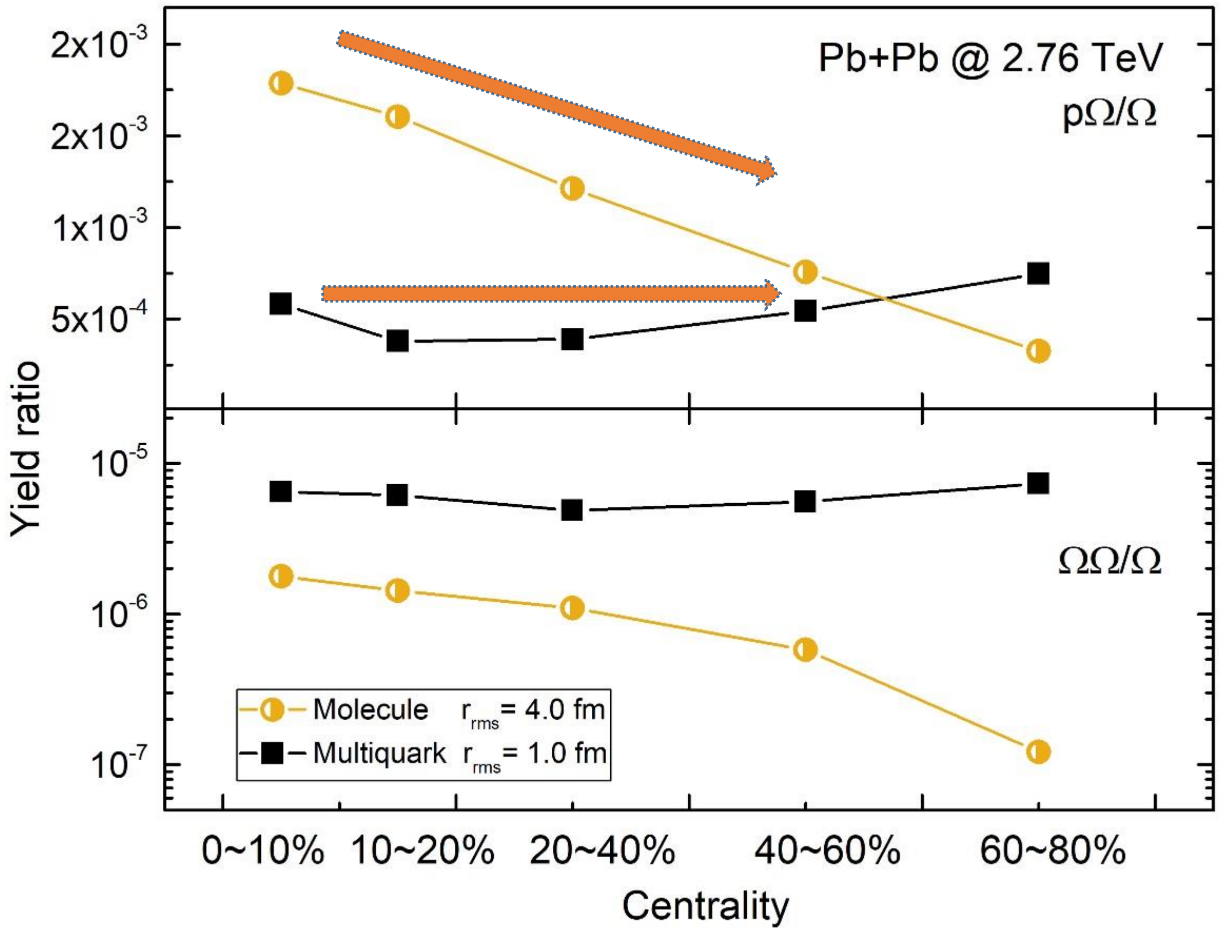

Distinct centrality dependence for molecular and multi-quark states!

Effects of hadronic re-scatterings via the kinetic approach

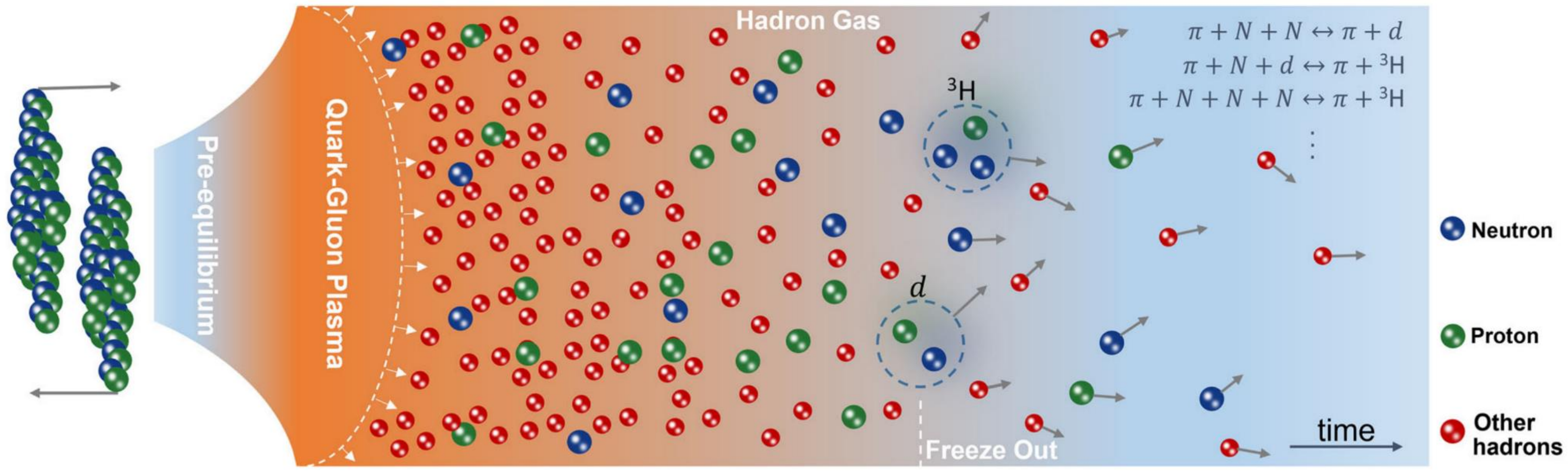

Dynamical modelling of light nuclei production

1991-1992

deuteron production ($NNN \leftrightarrow Nd$), P. Danielewicz, NPA533,712 (1991) , PLB274, 268 (1992)

2007-2009

deuteron production Oh & Ko, PRC 76, 054910 (2007); Oh, Lin & Ko, PRC 80, 064902 (2009)

deuteron production Cho & Lee, PRC 97, 024911 (2018)

$$\frac{dN_d(\tau)}{d\tau} = \sum_i \langle \sigma_{Ni} v_{Ni} \rangle n_i N_N(\tau) - \sum_i \langle \sigma_{di} v_{di} \rangle n_i N_d(\tau)$$

2018-2020

Vovchenko et al., PLB800, 135131(2020): Saha equation
Neidig et al., PLB 827, 136891 (2022): Rate equation

2019 deuteron production ($\pi NN \leftrightarrow \pi d$), Oliinychekov, Pang, Elfner & Koch, PRC 99, 044907 (2019) ; SMASH

2019-2024

Aichelin et al., PRC 101, 044905 (2019);
Coci et al., PRC 108, 014902 (2023)
Gläße et al., PRC 105, 014908 (2022):PHQMD
Kireyeu et al., PRC105, 044909 (2023): MST
Rais et al., PRC106, 064004(2022): 'formation' time
And more …

2021-2024

Kai-Jia Sun et al., Nat. Commun. 15, 1074 (2024); Hadronic rescat.
Rui Wang et al., PRC 108, L031601 (2023): Mott effects
$\pi NNN \leftrightarrow \pi t$…

Relativistic Kinetic Approach

P. Danielewicz et al., NPA533, 712 (1991); PLB274, 268 (1992);
Annals of Physics 152, 239(1984);

- Starting point is the two-nucleon Green's function
- $iG_2(x_1, x_2, t, x_1', x_2', t') =< T\{\psi(x_1,t)\psi(x_2,t)\psi^+(x_2',t')\psi^+(x_1',t')\} >$
- The deuteron occupation will be obtained from the function
- $iG_2^<(x_1, x_2, t, x_1', x_2', t') =< \psi^+(x_2',t')\psi^+(x_1',t')\psi(x_1,t)\psi(x_2,t) >$

Equation of motion of G_2 ⟹ Equation of motion of $G_2^<$ ⟹ Kinetic equation of f_2

$$\frac{\partial f_2}{\partial T} + \frac{\partial E}{\partial \boldsymbol{P}} \cdot \frac{\partial f_2}{\partial \boldsymbol{R}} - \frac{\partial E}{\partial \boldsymbol{R}} \cdot \frac{\partial f_2}{\partial \boldsymbol{P}} + \mathscr{D}' f_2 = \mathscr{K}^<(1+f_2) - \mathscr{K}^> f_2 . \qquad (2.23)$$

Including light nuclei size:

$$\frac{\mathrm{d}N_\nu}{\mathrm{d}\nu} = A \int \mathrm{d}T \int \mathrm{d}\boldsymbol{R}_1 \ldots \mathrm{d}\boldsymbol{R}_A \int \frac{\mathrm{d}\omega}{2\pi} \int \frac{\mathrm{d}\boldsymbol{p}_1}{(2\pi)^3} \cdots \frac{\mathrm{d}\boldsymbol{p}_A}{(2\pi)^3} 2\pi\delta(E_\nu - \omega - \epsilon_{p_2} - \ldots - \epsilon_{p_A})$$
$$\times (2\pi)^3 \delta(\boldsymbol{P}_\nu - \boldsymbol{p}_1 - \boldsymbol{p}_2 - \ldots - \boldsymbol{p}_A)(-\mathrm{i})\Sigma^<(\boldsymbol{p}_1, \omega; \boldsymbol{R}_1, T)$$
$$\times f(\boldsymbol{p}_2; \boldsymbol{R}_2, T) \ldots f(\boldsymbol{p}_A; \boldsymbol{R}_A; T) g_\nu(\tilde{\boldsymbol{p}}_1, \ldots, \tilde{\boldsymbol{p}}_{A-1}; \tilde{\boldsymbol{R}}_1, \ldots, \tilde{\boldsymbol{R}}_{A-1}) . \qquad (16)$$

Wigner function

Relativistic Kinetic Approach

K. J. Sun, R. Wang, C. M. Ko, Y. G. Ma, C. Shen, Nat. Commun. 15, 1074 (2024)

Relativistic kinetic equation for $\pi NN \leftrightarrow \pi d$

$$\frac{\partial f_d}{\partial t} + \frac{\mathbf{P}}{E_d} \cdot \frac{\partial f_d}{\partial \mathbf{R}} = -\mathcal{K}^{>} f_d + \mathcal{K}^{<}(1+f_d)$$

with collision integral:

$$\text{R.H.S.} = \frac{1}{2g_d E_d} \int \prod_{i=1'}^{3'} \frac{d^3\mathbf{p}_i}{(2\pi)^3 2E_i} \frac{d^3\mathbf{p}_\pi}{(2\pi)^3 2E_\pi} \frac{E_d d^3\mathbf{r}}{m_d}$$
$$\times 2m_d W_d(\tilde{\mathbf{r}}, \tilde{\mathbf{p}}) \left(\overline{|\mathcal{M}_{\pi^+ n \to \pi^+ n}|^2} + n \leftrightarrow p \right)$$
$$\times \Big[- \big(\prod_{i=1'}^{3'} (1 \pm f_i) \big) g_\pi f_\pi g_d f_d + \frac{3}{4} \big(\prod_{i=1'}^{3'} g_i f_i \big)$$
$$\times (1+f_\pi)(1+f_d) \Big] \times (2\pi)^4 \delta^4(p_{\text{in}} - p_{\text{out}})$$

Nonlocal collision integral to take into account the effects of finite nuclei sizes. W_d denotes deuteron Wigner function.

Impulse approximation (IA):

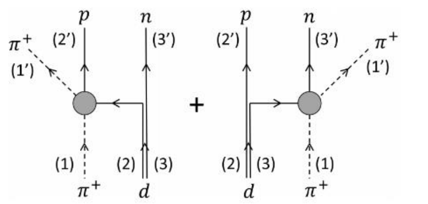

FIG. 1. Diagrams for the reaction $\pi^+ d \leftrightarrow \pi^+ np$ in the impulse approximation. The filled bubble indicates the intermediate states such as a Δ resonance.

Length/energy scale:

$\lambda_{thermal} \sim 0.5\ fm \ll r_{np} \sim 4\ fm$

Solving kinetic equations with the stochastic method using test particles

Probability for reaction $\pi d \leftrightarrow \pi NN$ to take place in volume ΔV and time interval Δt are given by

$$P_{23}|_{\text{IA}} \approx F_d v_{\pi^+ p} \sigma_{\pi^+ p \to \pi^+ p} \frac{\Delta t}{N_{\text{test}} \Delta V} + (p \leftrightarrow n),$$

$$P_{32}|_{\text{IA}} \approx \frac{3}{4} F_d v_{\pi^+ p} \sigma_{\pi^+ p \to \pi^+ p} \frac{\Delta t W_d}{N_{\text{test}}^2 \Delta V} + (p \leftrightarrow n)$$

For triton or helium-3:

$$P_{42}|_{\text{IA}} \approx \frac{1}{4} F_t \frac{v_{\pi N} \sigma_{\pi N \to \pi N} \Delta t}{N_{\text{test}}^3 \Delta V} W_t$$

'renormalization' factor F_d, F_t which can be fixed by πd and πt cross sections.

Validation: Box calculation

K. J. Sun, R. Wang, C. M. Ko, Y. G. Ma, C. Shen, Nat. Commun. 15, 1074 (2024)

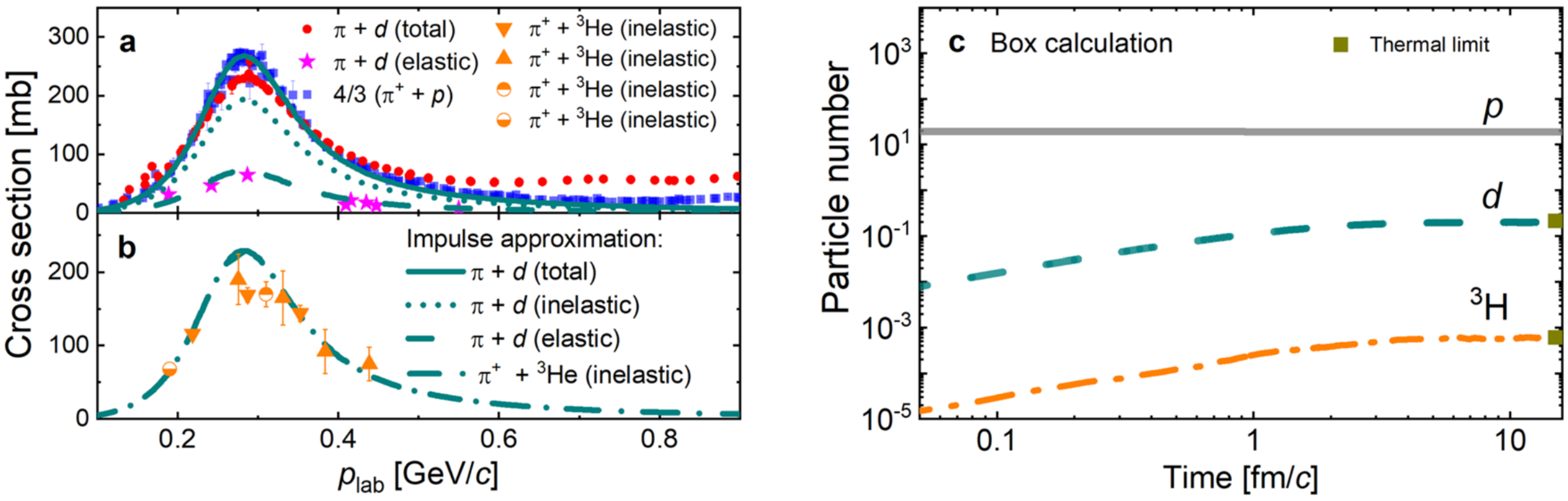

Hadronic re-scattering effects at RHIC

K. J. Sun, R. Wang, C. M. Ko, Y. G. Ma, C. Shen, Nat. Commun. 15, 1074 (2024)
Data from STAR, PRL 130, 202301 (2023)

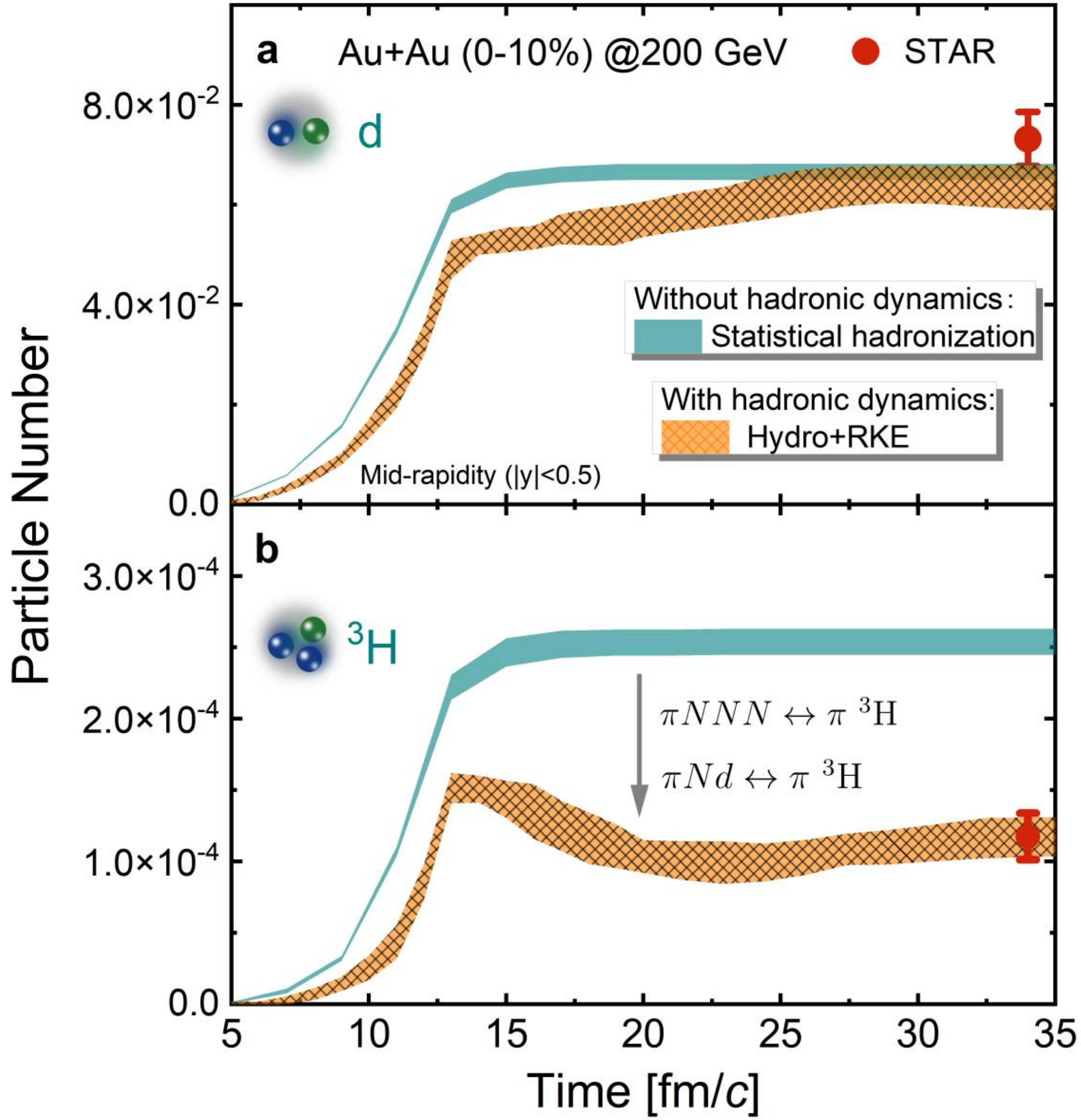

- A = 2 $\pi NN \leftrightarrow \pi d$, $NNN \leftrightarrow Nd$
- A = 3 $\pi NNN \leftrightarrow \pi t(h)$, $\pi Nd \leftrightarrow \pi t(h)$, $NNNN \leftrightarrow Nt(h)$, $NNd \leftrightarrow Nt(h)$, and etc.

Hadronic re-scattering effects at RHIC

K. J. Sun, R. Wang, C. M. Ko, Y. G. Ma, C. Shen, Nat. Commun. 15, 1074 (2024)
Data from STAR, PRL 130, 202301 (2023)

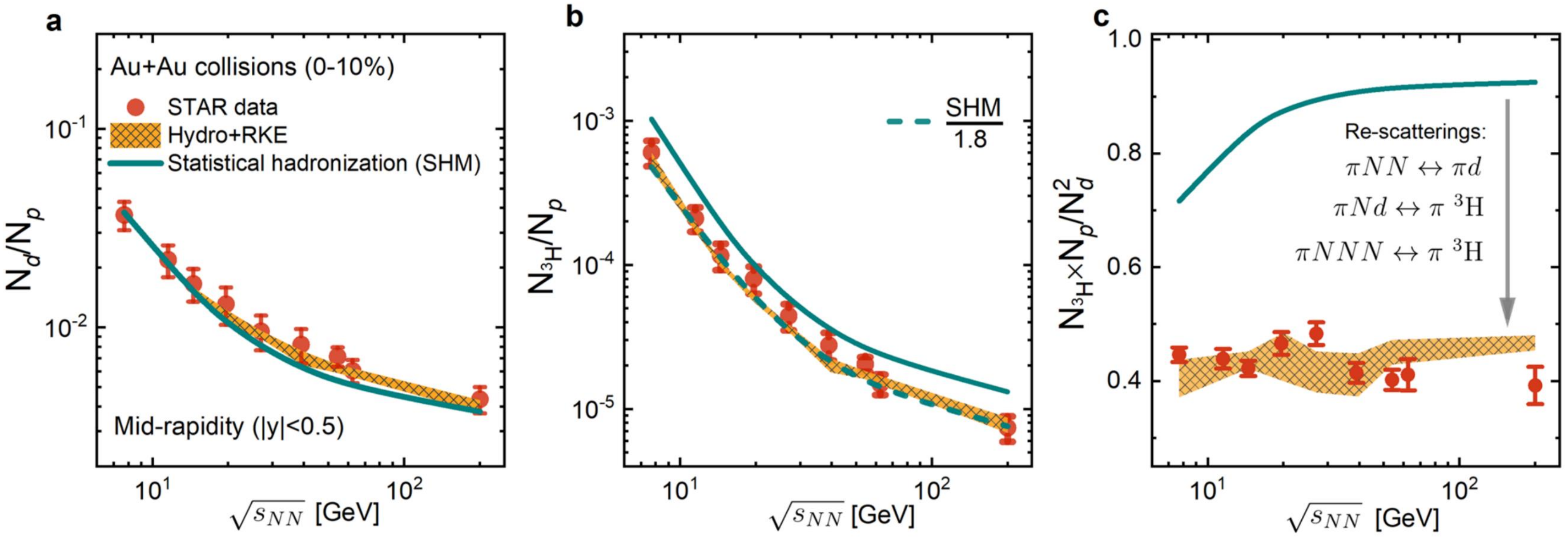

Hadronic re-scatterings have small effects on the final deuteron yields (see also D. Oliinychenko et al. PRC 99, 044907 (2019)), but they reduce the triton yields by about a factor of 1.8.

Hadronic re-scattering effects at the LHC

K. J. Sun, R. Wang, C. M. Ko, Y. G. Ma, C. Shen, Nat. Commun. 15, 1074 (2024)
Data from ALICE, Phys. Rev. C 107, 064904 (2023)

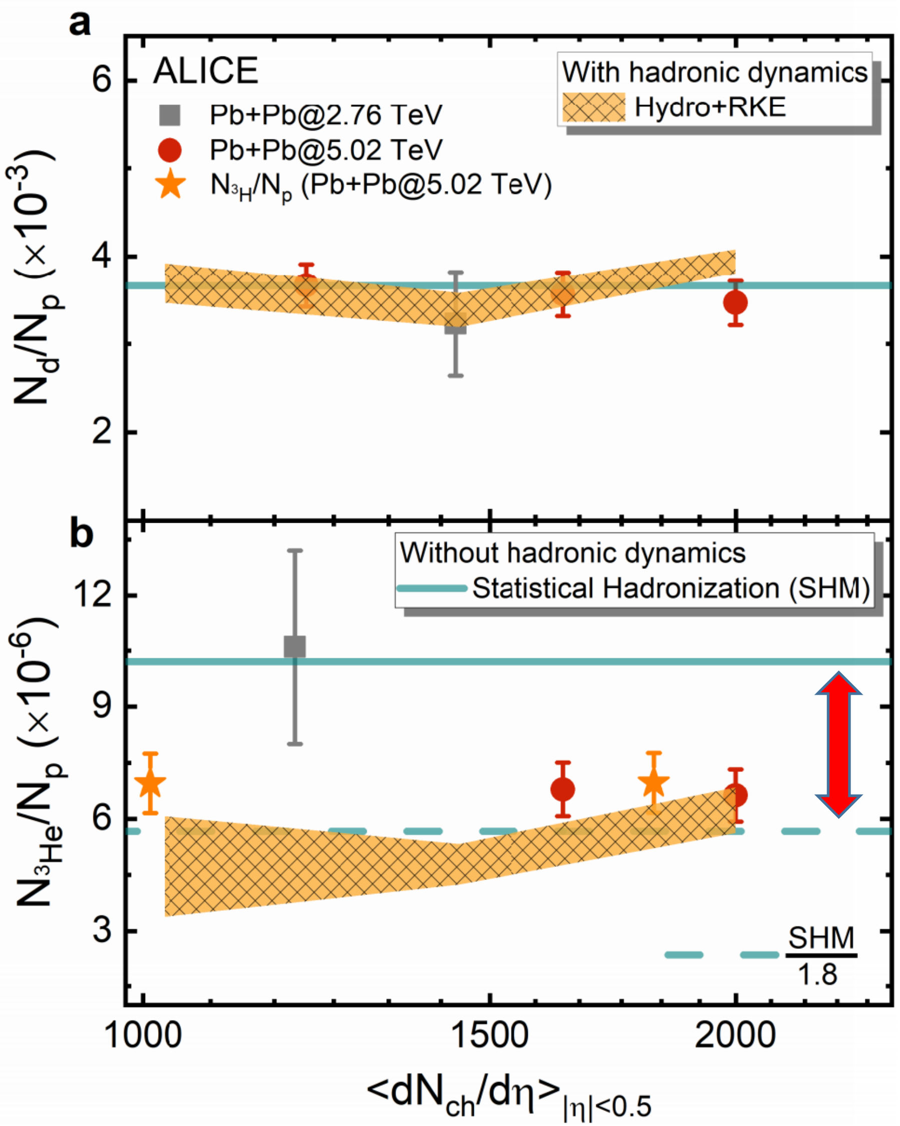

Similar strong hadronic effects occur at the LHC energies.

Mott effects at large baryon densities

Light nuclei production in intermediate energies

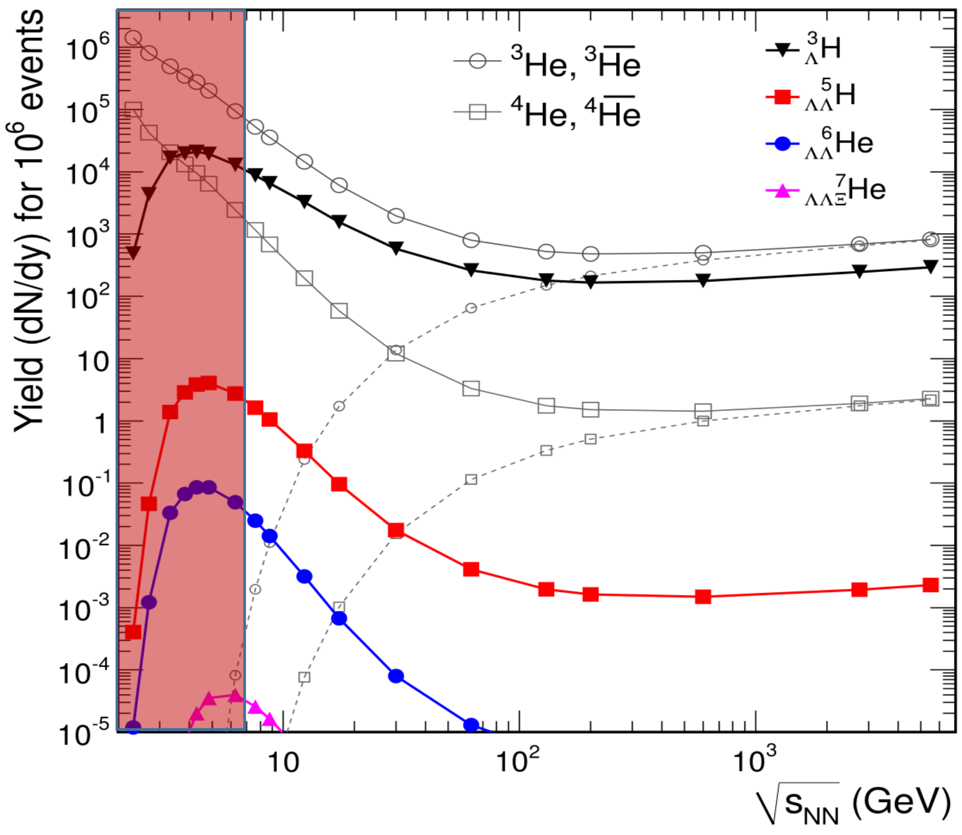

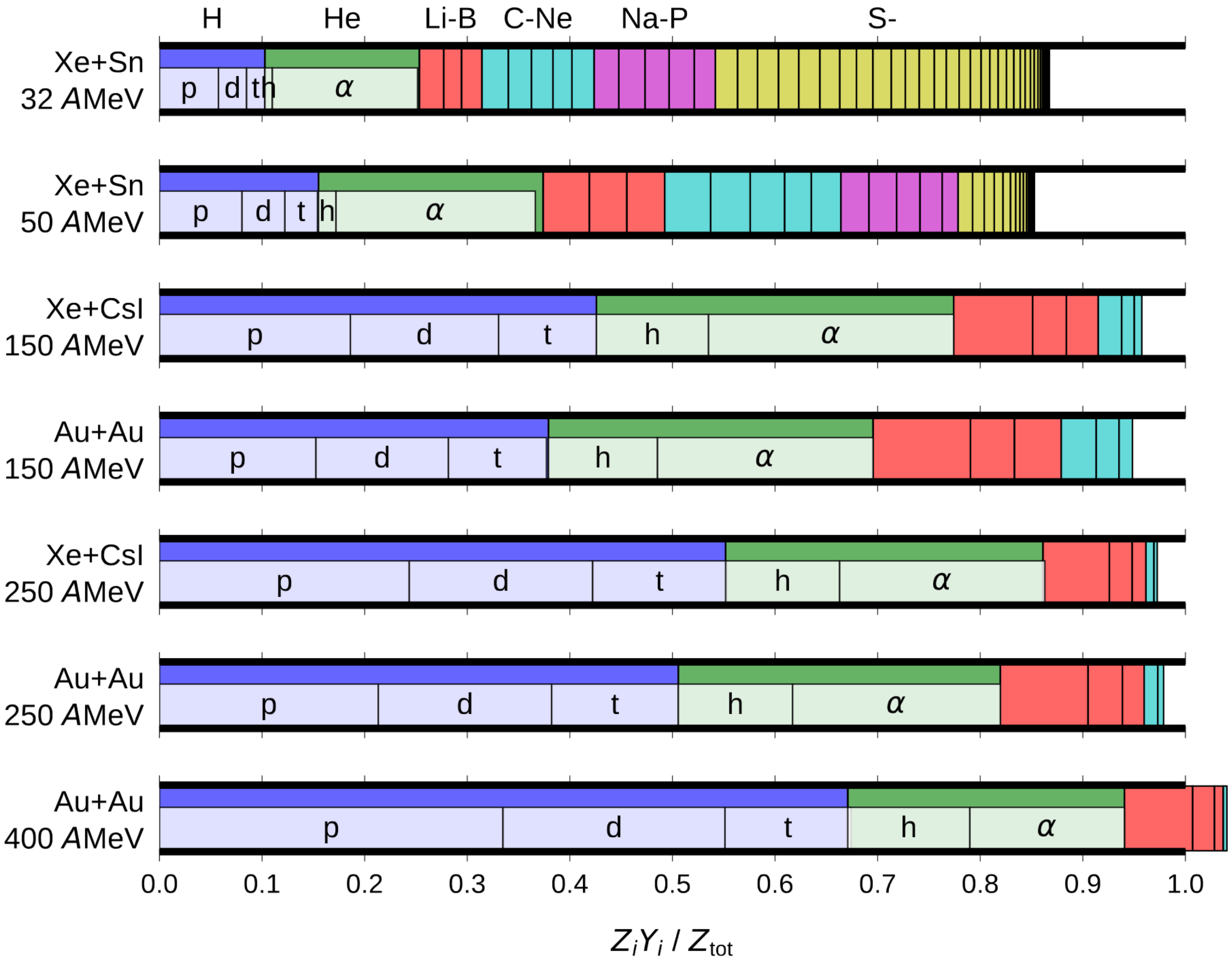

Light nuclei are **abundantly** produced.

More alpha-particle than helium-3 !

A. Andronic et al., Phys. Lett. B697, 203 (2011)
A. Ono, PPNP 105, 139-170 (2019)
FOPI Collaboration, Nucl. Phys. A848, 366-427 (2010)
INDRA data: Phys. Rev. C 67, 064613 (2003)

Pauli Blocking and Mott Effect

G. Röpke et al., Nucl. Phys. A379, 536 (1982)

S. Typel et al., Phys. Rev. C81, 015803 (2010)

C. Kuhrts, Phys. Rev. C63, 034605 (2011)

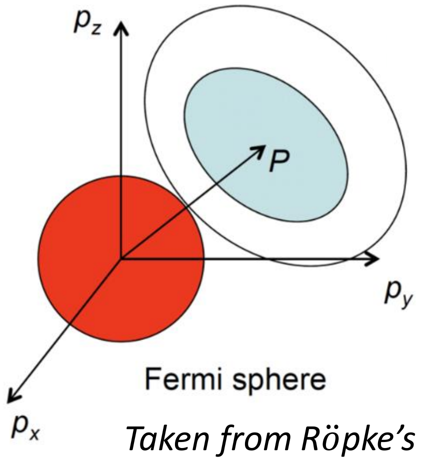

Taken from Röpke's talk

Mott effect: a light nucleus becomes unbound if the phase-space density of its surrounding nucleons are too large.

Binding energy for P = 0 GeV/c light nuclei

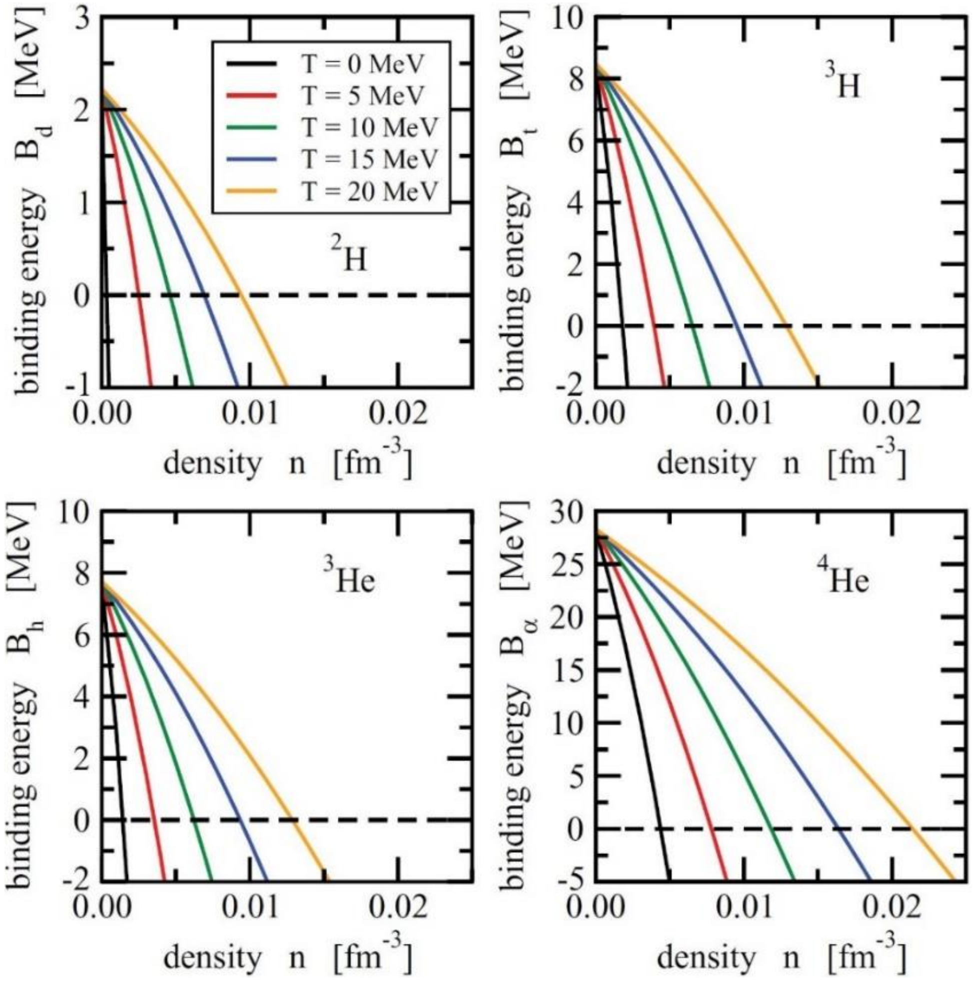

$$\int d^3q\, f(q + \frac{P_{\rm c.m.}}{2})\, |\phi(q)|^2 \leq F_{\rm cut}$$

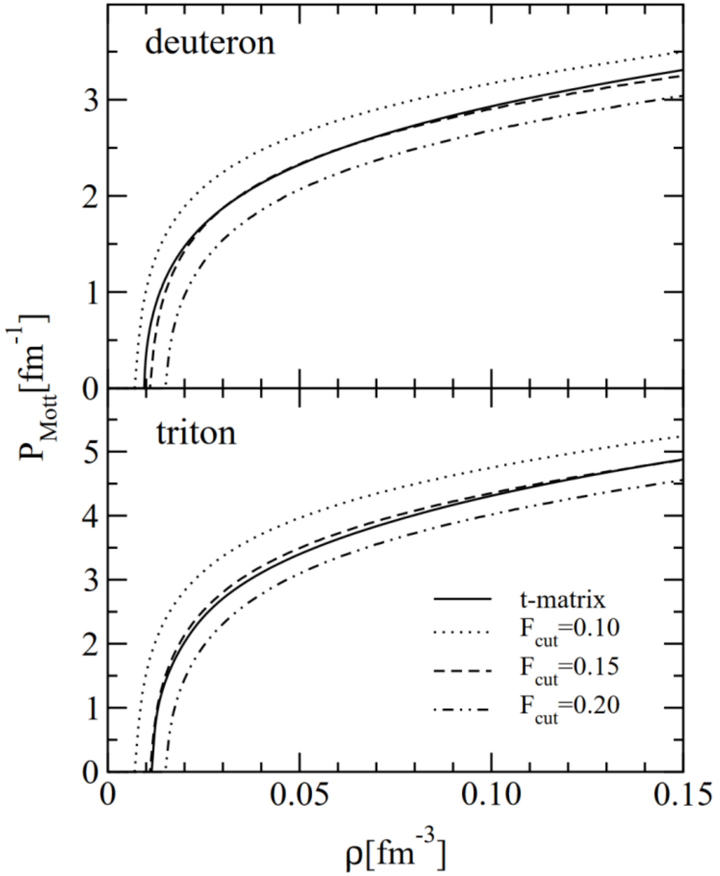

Mott Effect

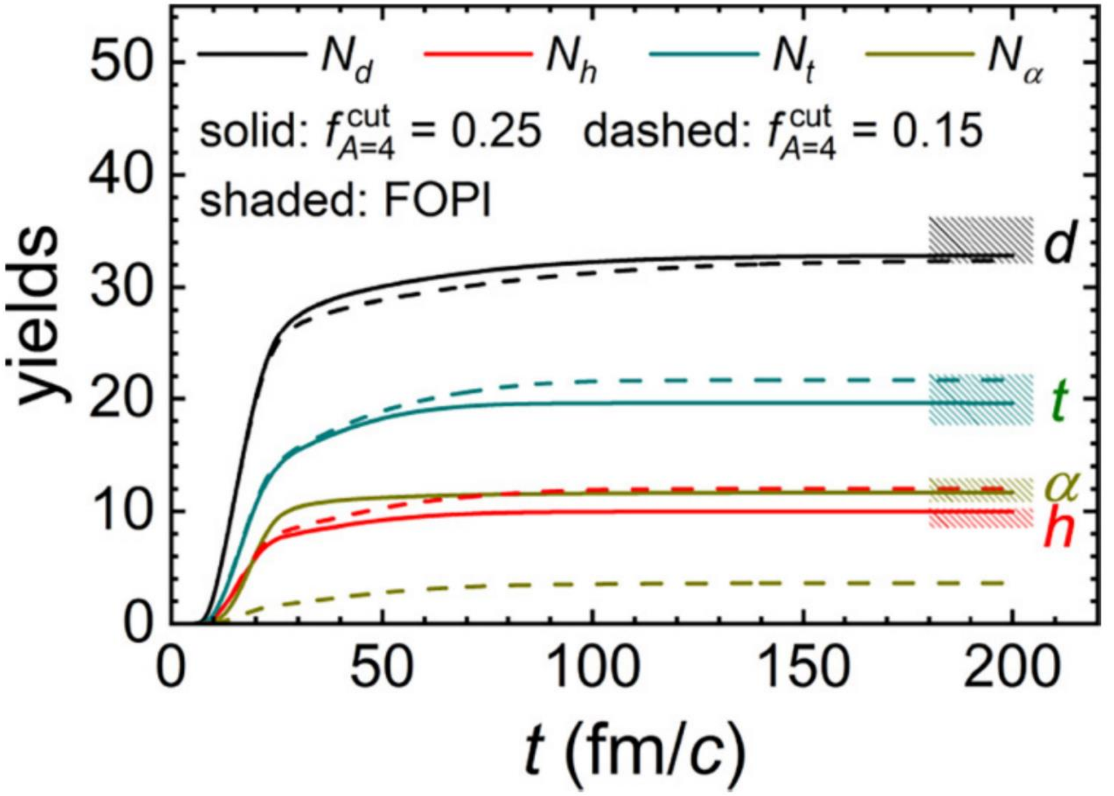

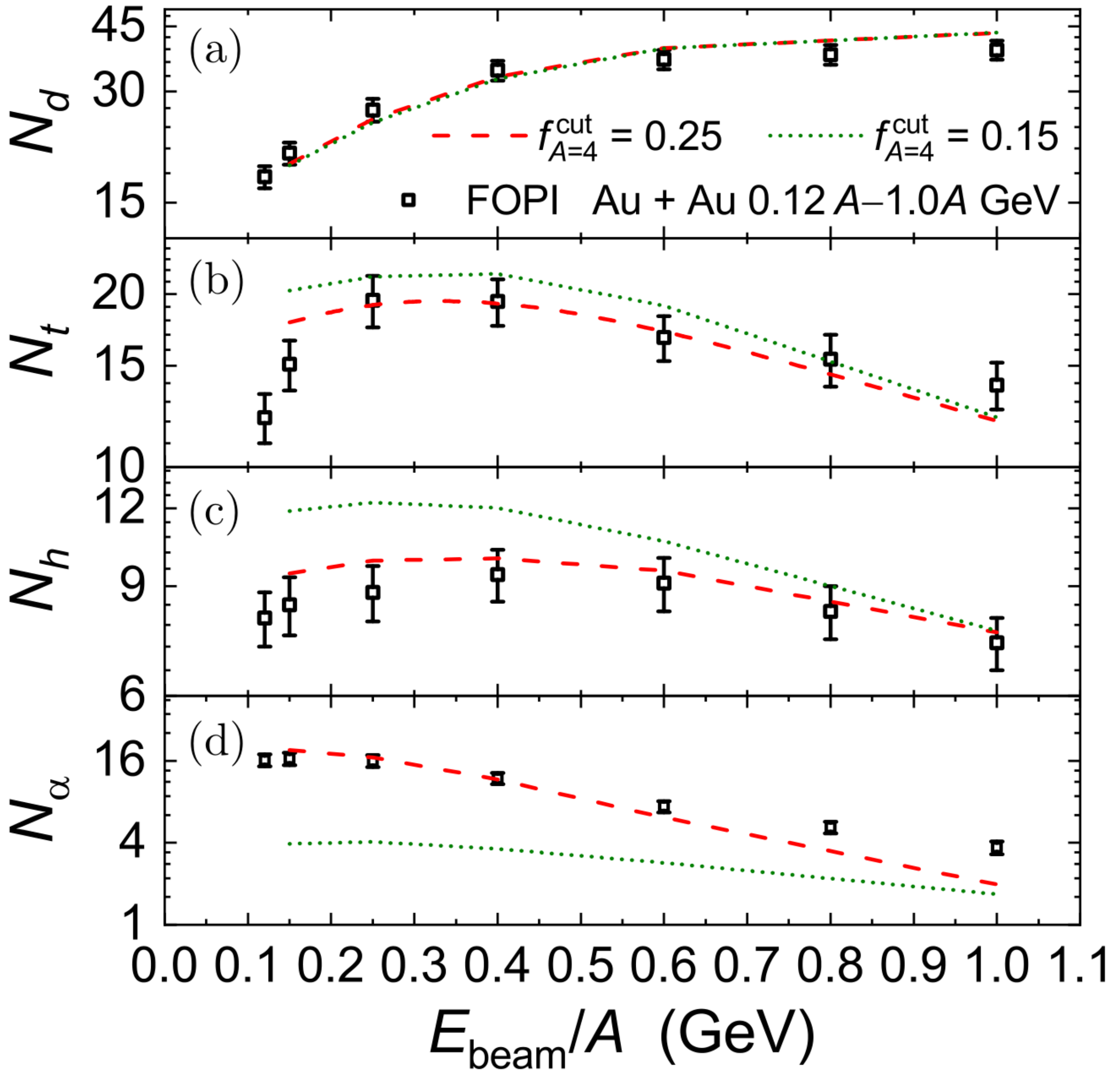

R. Wang, Y. G. Ma, L. W. Chen, C. M. Ko, K. J. Sun, and Z. Zhang, PRC 108, L031601 (2023)

Summary and outlook

1. The little-bang nucleosynthesis is relevant to many fundamental physics.
   A general thermal pattern is observed (e.g. central AA)
2. Quantum correction: In collisions of small systems, light (hyper)nuclei production are suppressed due to their appreciable sizes.
3. Hadronic effects: Post-hadronization dynamics plays a vital role in the little-bang nucleosynthesis. It suppresses triton yields by about a factor of two at RHIC and LHC energies. (confirmed in STAR and ALICE measurements)
4. Mott effects: Light nuclei yields are reduced in the medium due to Pauli blocking.
5. Hopefully, we will have a fully quantum-mechanical description of the dynamics of little-bang nucleosynthesis in the near future.

Backup

‘Formation’ time

J. Rais, H. Hees, and C. Greiner, Phys. Rev. C 106, 064004 (2022)

$$\tau_{\mathrm{f}} \sim \frac{\hbar}{E_{\mathrm{D}}} \quad \text{or} \quad \tau_{\mathrm{f}} \sim \frac{\hbar}{E_{\mathrm{B}}}, \tag{22}$$

where τ_{f} is then the “formation time” of for example a deuteron, and E_{D} the energy difference of a certain state before and after the interaction or even simply the binding energy, E_{B}.

In contradiction to this possible straight-forward idea, as demonstrated in fig. 19 and fig. 20, the states form immediately, independently of the pulse duration (cf. also fig. 4-fig. 7). Especially in fig. 19 we decrease the pulse duration to only 0.1 fm (pink line) and find, that still the state reacts immediately to the pulse.

Therefore, as illustrated by these results, Heisenberg’s uncertainty relation in energy and time should be understood in a different way. It is more suitable to talk about the population time instead of the formation time, because we want to point out, that the formation time is equivalent to the interaction time of the potential, and therefore the term is misleading. This picture is also in good agreement with the interpretation of the energy-time uncertainty relation given in [27] and [29], which is motivated by considering the transition probability from the energy eigenstate ψ_i to the energy eigenstate ψ_f of the unperturbed system, due to the external potential. In first-order perturbation theory the transition amplitude is given by eq. (21), which reads, rewritten for our present case of a potential (17) representing only one pulse

No time delay: The formation of states is not delayed due to the uncertainty relation, but basically follows the pulse shape of the acting perturbation.

Hadronic Re-scattering Effects

$\pi NN \leftrightarrow \pi d$

D. Oliinychenko, et al., PRC99, 044907 (2019)

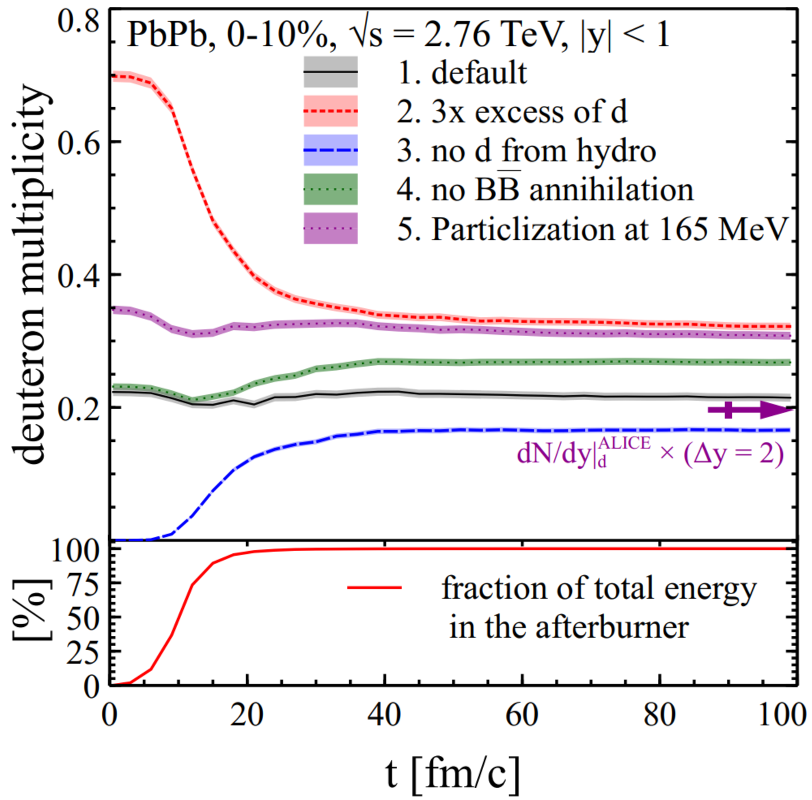

V. Vovchenko, et al., PLB800, 135131 (2020)

T. Neidig, et al., PLB827, 136891 (2022)

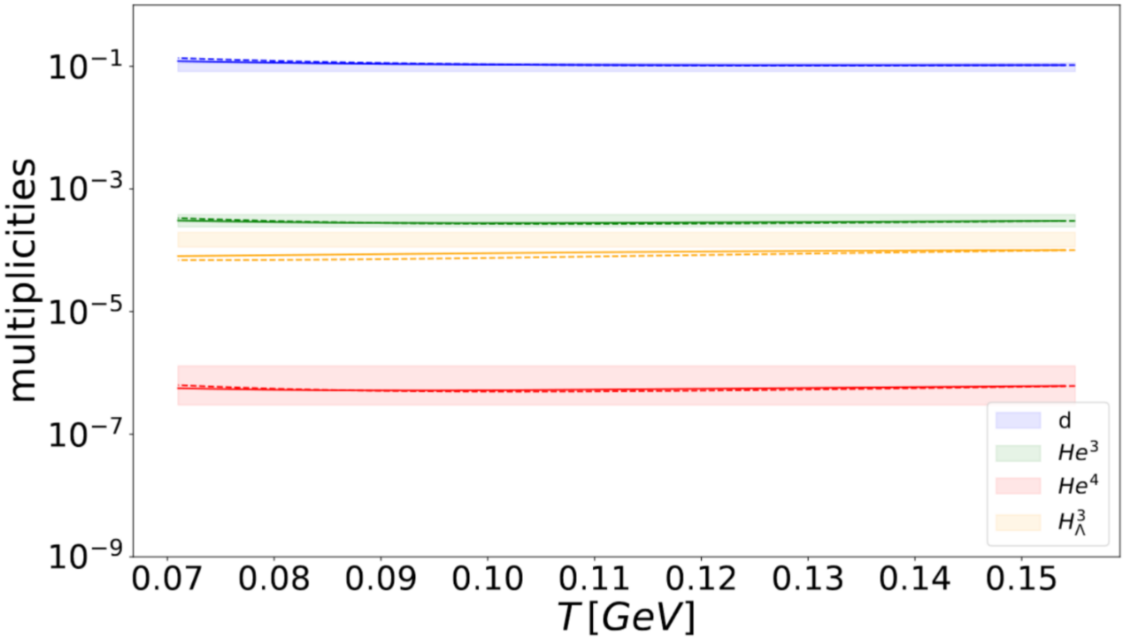

The obtained hadronic effects on light nuclei production are small

The Triton 'Puzzle' at RHIC

STAR, Phys. Rev. Lett. 130 (2023) 202301

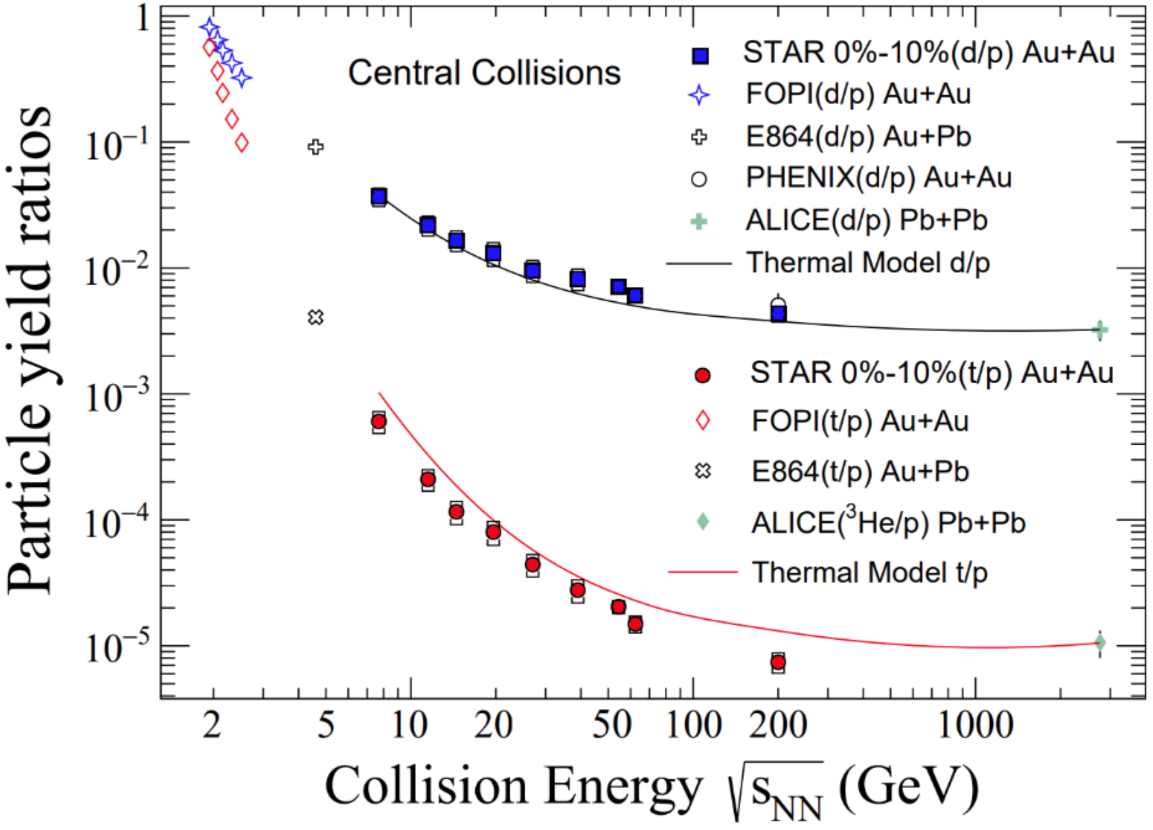

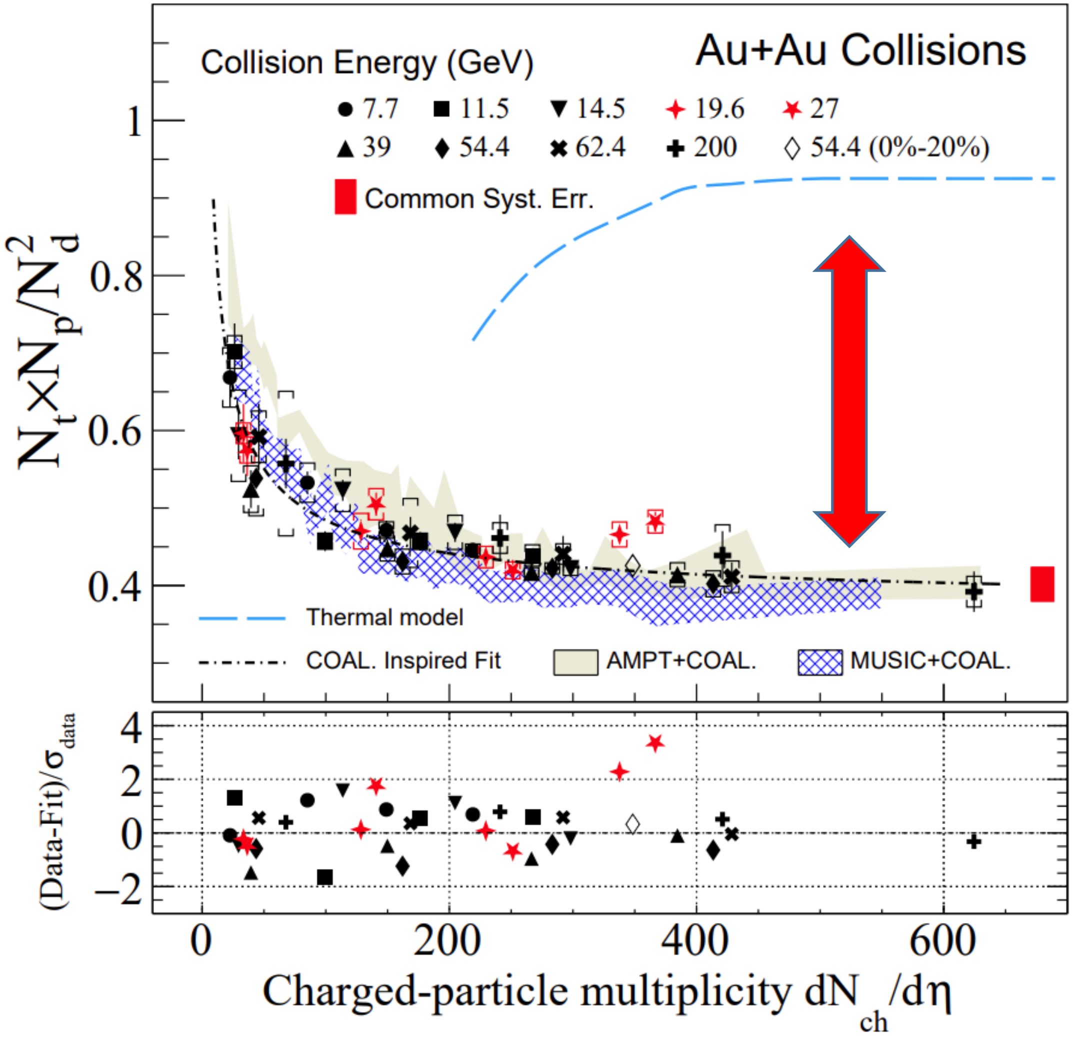

Triton yields at RHIC are overestimated by the statistical hadronization model.

The Triton ‘Puzzle’ at LHC

ALICE, Phys. Rev. C 107, 064904 (2023)

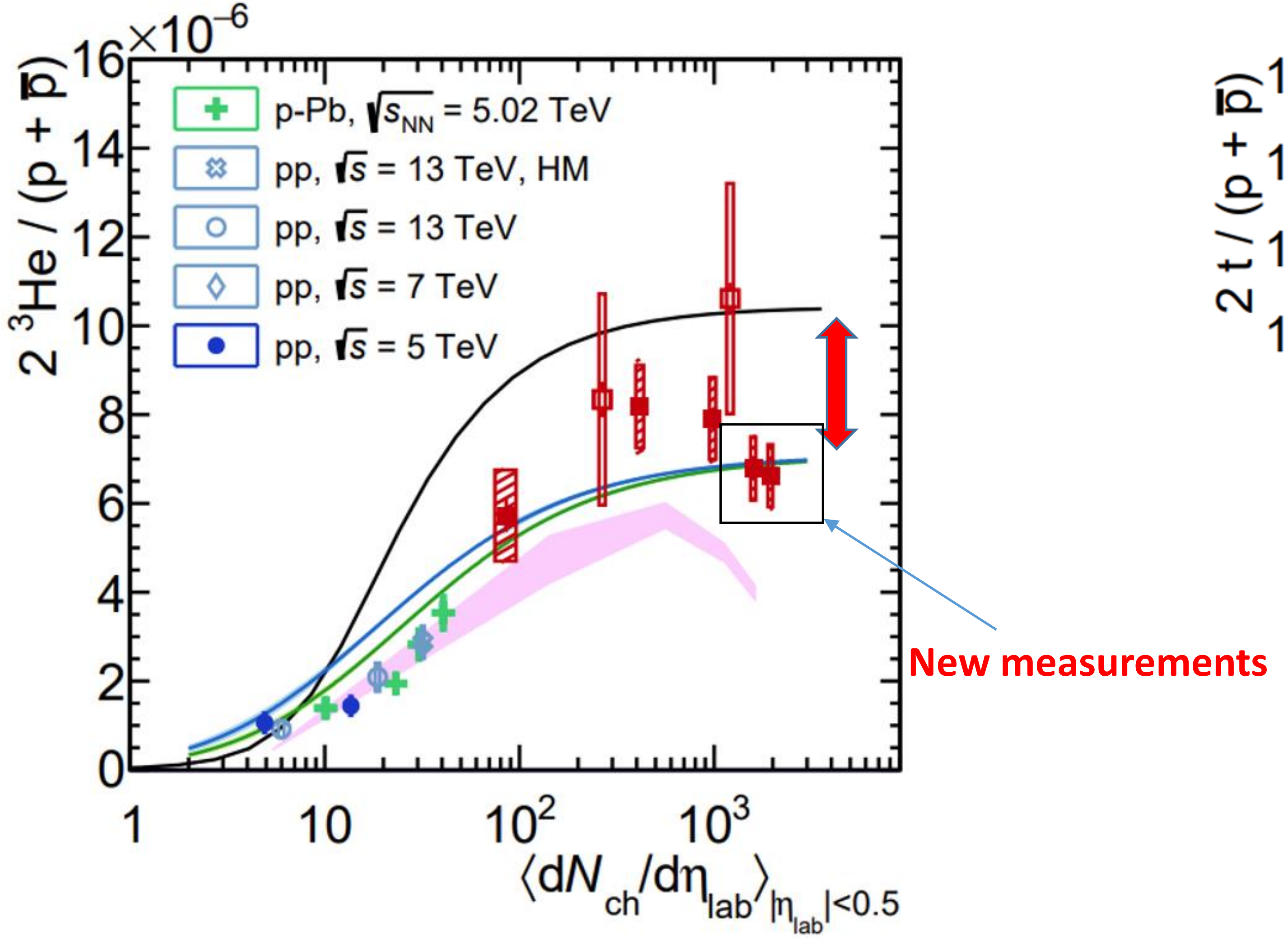

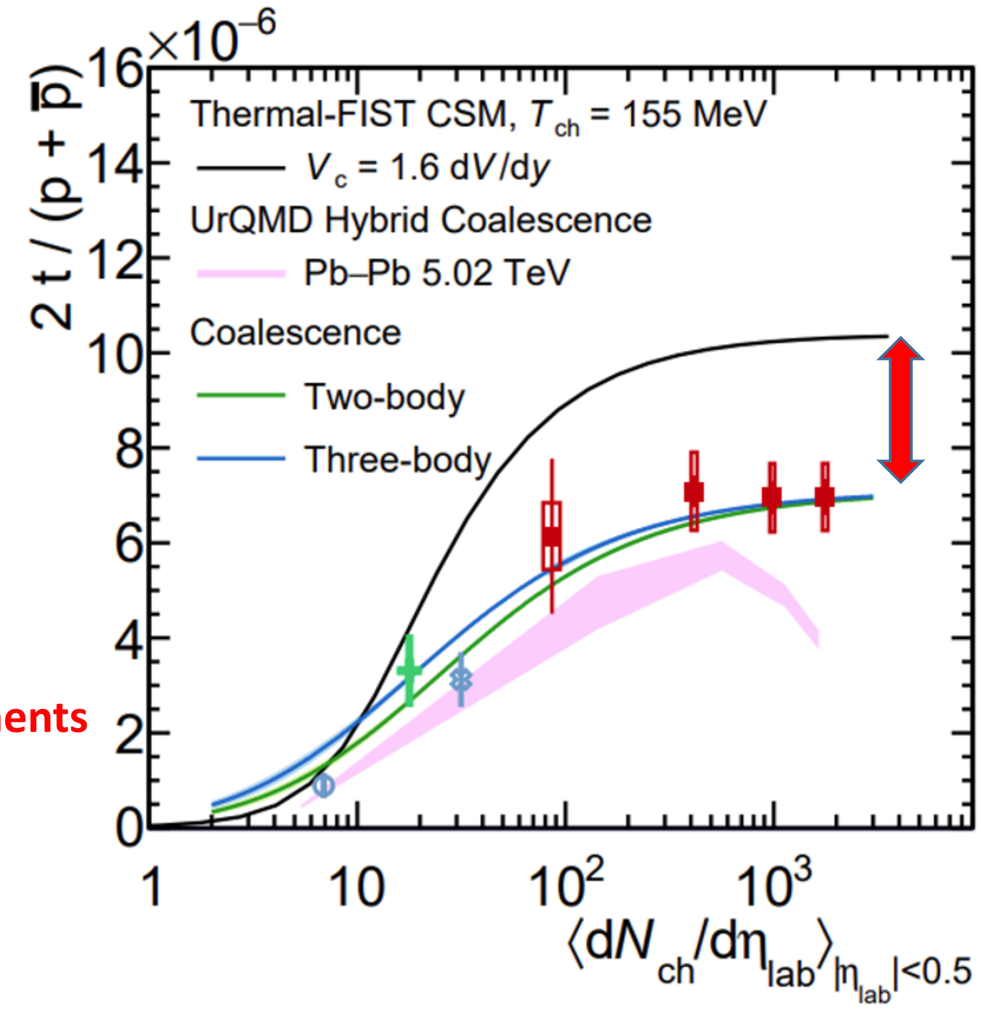

Triton (helium-3) yields at LHC are overestimated by the statistical hadronization model.